NASA Contractor Report 172325

NASA-CR-172325
19840015858

FINITE ELEMENT ANALYSIS OF WRINKLING MEMBRANES

Richard K. Miller, John M. Hedgepeth,
Victor I. Weingarten, Prasanta Das,
and Shahrzad Kahyai

UNIVERSITY OF SOUTHERN CALIFORNIA
Los Angeles, California 90089

Grant NAG1-235
April 1984

National Aeronautics and
Space Administration

Langley Research Center
Hampton, Virginia 23665

26 1 1 RN/NASA-CR-172325
DISPLAY 26/2/1
84N23926*# ISSUE 14 PAGE 2158 CATEGORY 39 RPT#: NASA-CR-172325 NAS 1.26:172325 USC-CE-83-05 CNT#: NAG1-235 84/04/00 86 PAGES
UNCLASSIFIED DOCUMENT
UTTL: Finite element analysis of wrinkling membranes
AUTH: A/MILLER, R. K.; B/HEDGEPETH, J. M.; C/WEINGARTEN, V. I.; D/DAS, P.; E/KAHYAI, S. PAA: B/(Astro Research Corp.)
CORP: University of Southern California, Los Angeles. CSS: (Dept. of Civil Engineering.) AVAIL.NTIS SAP: HC A05/MF A01
MAJS: /*ALGORITHMS/*FINITE ELEMENT METHOD/*MEMBRANES/*NONLINEARITY/*STRESS ANALYSIS/*WRINKLING
MINS: / COMPUTER PROGRAMS/ CURVATURE/ DEFORMATION/ DISPLACEMENT/ FLATNESS/ ITERATION/ PROBLEM SOLVING
ABA: Author
ABS: The development of a nonlinear numerical algorithm for the analysis of stresses and displacements in partly wrinkled flat membranes, and its implementation on the SAP VII finite-element code are described. A comparison of numerical results with exact solutions of two benchmark problems reveals excellent agreement, with good convergence of the required iterative procedure. An exact solution of a problem involving axisymmetric deformations of a partly wrinkled shallow curved membrane is also reported.

ENTER:

TABLE OF CONTENTS

TABLE OF CONTENTS (Cont.)

I. INTRODUCTION

Many structural concepts for large spacecraft applications involve a tensioned membrane surface. Since much of the structural weight in such spacecraft is associated with compression members necessary to equilibrate the membrane tension, a high premium is placed on designing structures with extremely small membrane tension. As a result, the elastic strains in the membrane may well be much smaller than anticipated thermal strains, so that a high likelihood exists for the development of wrinkled and slack regions within an otherwise taut membrane surface. The existence and severity of such wrinkled regions may have an adverse effect on the overall elastic stability of the spacecraft, as well as on the intended spacecraft performance if the membrane surface acts as a reflector with stringent requirements for geometrical accuracy of the surface. Thus, the problem of predicting the stresses and displacements within a partly wrinkled membrane surface is one of some current technological interest in the aerospace industry.

In spite of the importance of the mechanics of wrinkling behavior of membranes the field remains largely unexplored. Apparently the earliest investigation in the field was reported more than 50 years ago by Wagner [1] who conceived "tension field theory" in order to explain the behavior of thin metal webs in beams and spars carrying a shear load well in excess of the initial buckling value. Wagner's method of analysis was based on lengthy geometrical considerations. Reissner [2] and independently Kondo [3] developed a simpler analysis based on straight-forward calculus, and presented the first exact solutions to problems involving a non-repetitive pattern of tension rays. Iai [4] developed an analysis procedure based on a principle of maximum strain energy under given boundary displacements.

This, and subsequent Japanese work on tension fields is well documented in a review paper (in English) by Kondo, Iai, Moriguti and Murasaki [5].

In a series of more recent papers, Mansfield [6-9] developed an analysis procedure which combines the "tension ray" concepts of Reissner and Kondo and a principle of Maximum "tension" strain energy similar to that of Iai. The first of his papers [6] developed an analogy with inextensional plate deformation theory, and worked example problems involving shearing and lateral contraction of membrane strips, and torsion of an annular membrane. Later [7], this work was extended to consider problems of load transfer from an elastic rod bonded to a flat membrane strip. Experiments were also reported which confirm predictions of the theory. Next [8], the analysis was generalized to include anisotropic and nonlinear membrane behavior typical of woven and fiberous materials. It was shown that such nonlinearities tend to amplify stress concentrations at corners and at the ends of a cut. Finally [9], the curved winkle patterns within hanging slack membranes was analyzed for various shapes of membranes and various support conditions. The curved wrinkles were shown to be governed by a one-dimensional diffusion equation and an analogy with heat conduction in a slab was noted.

All the published work just cited considers static stresses and small deformations within fully-wrinkled flat membranes. A generalization to arbritrarily large deformations, with particular concern for the behavior of stretching skin, was recently presented by Danielson and Natarajan [10]. More recently, Wu [11] considered membrane wrinkling in the neighborhood of a sutured hole. Then Wu and Canfield [12] presented a general finite plane-stress analysis for wrinkling of flat membranes.

However, for applications in space structures, a particularly important class of problems is that of partly wrinkled membranes. Such membranes contain both wrinkled and taut regions. A general theory for partly wrinkled membranes was developed by Stein and Hedgepeth [13] some 20 years ago. Their approach is based on experimental observations which show that when wrinkles develop within a membrane parallel to, say, the x-direction, the associated overall contraction in the y-direction exceeds that predicted by the Poisson's ratio effect. The additional average normal strain in the y-direction may be regarded as an "average wrinkle strain". For purposes of simplified analysis, these geometric features of wrinkling were incorporated in Ref. 13 into a Hookean material model by appropriately increasing the local effective value of Poisson's ratio in wrinkled regions. This effective value of Poisson's ratio may be determined by imposing the approximation that the local state of stress in a wrinkled region is one of uniaxial tension. The resulting theory retains the simplicity of form of the linear governing equations of elasticity, with the additional feature that the material parameters are dependent upon the local state of strain. Comparisons between the predictions of this theory and experimental results for some simple configurations [13,14,15] show that very satisfactory results may be obtained. Furthermore, of the available theories for wrinkling of membranes, the Stein-Hedgepeth theory appears particularly promising for finite element implementation. Recently [16], the approach was used to construct an algorithm for finite element analysis of flat membranes which contain taut, wrinkled, and slack regions.

With regard to curved membranes containing wrinkled regions, apparently the earliest work was done by Taylor [17] more than 60 years ago, in an analysis of parachute shapes. Taylor analyzed the geometry and stresses within a parachute formed from an initially flat circular membrane by imposing the condition of zero hoop stress, and ignoring the stretching of the membrane near the crown. An extension of Taylor's work was presented more recently for isotensoid surfaces by Houtz [18] and Mikulas and Bohon [19].

An analysis of axisymmetric doubly curved membranes which are formed from an intially flat membrane was presented by Mikulas [20]. The analysis allows stretching of the membrane surface near the crown to remove wrinkles, and includes a wrinkled region near the outer edge. The taut region near the crown is analyzed by a nonlinear membrane theory [21] based on Sander's theory of thin shells [22] with the omission of the bending terms. The wrinkled region near the outer edge is analyzed by imposing the zero hoop stress condition introduced by Taylor. Application is made to three example problems, including the pressurization of a pleated flat circular membrane attached to a rigid circular rim, the stretching of an initially flat circular membrane over a doubly curved, axisymmetric rigid mandrel, and the very large deformation behavior of a pressurized membrane cylinder subjected to a radial line load.

Although it is not the primary focus of the reported research, the work of Zak on wave propagation within and vibration of partly wrinkled membranes is noteworthy. In a series of papers [23-30] Zak considers the stress conditions for local buckling within a thin membrane, and develops a continuum model for the propagation of shock waves, and "snaps" within thin membrane surfaces. His continuum theory for in-plane motion ignores the kinetic erergy of the out-of-plane motion in wrinkled regions, and results in an in-plane equation of motion which displays variable mass characteristics. As a result, his

theory predicts a "damping" out of in-plane vibrations as the kinetic energy of the in-plane motion is converted into out-of-plane motion through shocks. Examples include a proof that static wrinkle patterns in fully wrinkled flat sheets loaded only along their edges must be straight lines. Also, one dimensional examples involving shock wave propagation in a freely hanging string, and vibrations of a single-degree-of-freedom oscillator constrained by an inextensible string are presented.

Presented in this report are the results of one year of research supported by the National Aeronautics and Space Administration under Grant Number NAG-1-235 regarding the finite element analysis of wrinkling membranes. The research was performed at the University of Southern California (USC) in the Department of Civil Engineering, with technical assistance from Dr. John M. Hedgepeth of Astro Research Corporation of Carpinteria, California.

Chapter two of this report presents the results of an analysis and exact solution for a problem involving axisymmetric deformations of a shallow curved membrane. The problem was considered in order to provide an exact solution and "benchmark" for calibration of future numerical examples.

Chapter three describes the implementation of the numerical algorithm recently developed by Miller and Hedgepeth [16] on the SAP VII finite element code at USC. Chapters four and five then present an evaluation of this algorithm. The evaluation is based on a comparison of analytical and numerical results for stresses and displacements in two benchmark problems involving a partly wrinkled flat membrane. These comparisons

reveal a high degree of accuracy for the finite element algorithm. Furthermore, convergence of the required iterative procedure in this nonlinear problem was achieved without excessive computation.

II. AXISYMMETRIC DEFORMATION OF SHALLOW MEMBRANE

2.1 General Analysis

Consider a shallow pressurized membrane of spherical radius a. For axisymmetric loading, the equilibrium equations are

$$\left.\begin{aligned} \frac{d}{dr}(rN_r) &= N_\theta \\ \frac{d}{dr}\left(r^2 N_{r\theta}\right) &= 0 \\ N_r\left(\frac{r}{a} - \frac{dw}{dr}\right) &= \frac{P}{2\pi r} + \frac{pr}{2} \end{aligned}\right\} \qquad (1)$$

where N_r, N_θ, and $N_{r\theta}$ are the usual stress resultants, r is the radial dimension, p is the internal pressure, and P is an added center vertical load.

The strain-displacement relations are

$$\left.\begin{aligned} \varepsilon_r &= \frac{du}{dr} + \frac{w}{a} + \frac{1}{2}\left(\frac{dw}{dr}\right)^2 \\ \varepsilon_\theta &= \frac{u}{r} + \frac{w}{a} \\ \gamma_{r\theta} &= r\,\frac{r}{dr}\left(\frac{v}{r}\right) \end{aligned}\right\} \qquad (2)$$

where u and v are the radial and circumferential tangential displacements, and w is the normal displacement. We have assumed small strains and small slopes in comparison to unity except for the second-order term in the expression for ε_r; this is necessary to be consistent with the displacement-dependent term in the third of Eqs. (1). Also, Eqs. (1) and (2) are valid only for r<<a inasmuch as they apply to "shallow" configurations.

We are interested in solving the equations for an inextensional membrane both wrinkled and unwrinkled. In an unwrinkled region, then

$$\varepsilon_r = \varepsilon_\theta = \gamma_{r\theta} = 0$$

In addition, in order that the principal stresses be non-negative, the stresses must obey the inequality

$$N_r N_\theta > N_{r\theta}^2$$

On the other hand, in a wrinkled region,

$$N_r N_\theta = N_{r\theta}^2$$

and

$$\frac{\varepsilon_r}{\varepsilon_\theta} = \frac{N_\theta}{N_r}$$

The latter condition arises from the facts that the principal tension is parallel to the wrinkles, and the principal strain is perpendicular to them.

Consider the annular region between $r = r_0$ and $r = r_1$. Let $w = u = v = 0$ at $r = r_1$, and let the load P and moment Q be applied to the "rigid" plug occupying the center. For small P and Q, there will be no wrinkles; for large P and Q, the entire annulus will be wrinkled. For intermediate values, the innter part of the annulus will be wrinkled, and the outer portion will be unwrinkled.

In all cases, the second of Eqs. (1) can be integrated to yield

$$N_{r\theta} = \frac{Q}{2\pi r^2}$$

$$= \left(\frac{r_0}{r}\right)^2 N_{r\theta_0} \qquad (4)$$

where

$$N_{r\theta_0} = \frac{Q}{2\pi r_o^2}$$

is the shear stress at the inner boundary.

2.2 Unwrinkled Region

For the unwrinkled region, the displacements must represent rigid-body motion. Thus,

$$u = v = w = 0$$

Solving the third of Eqs. (1) gives

$$\bar{N}_r = 1 + \frac{\bar{P}}{\rho^2} \tag{6}$$

The first of Eq. (1) then yields

$$\bar{N}_\theta = 1 - \frac{\bar{P}}{\rho^2} \tag{7}$$

where the various quantities have been nondimensionalized as follows:

$$\bar{N}_{r,\theta} = \frac{2}{pa} N_{r,\theta}$$

$$\bar{P} = P/(\pi r_o^2 p)$$

$$\bar{Q} = Q/(\pi r_o^2 ap)$$

$$\rho = r/r_o$$

In order that the membrane be unwrinkled

$$\bar{N}_r \bar{N}_\theta > \bar{N}_{r\theta}^2$$

or

$$\rho^4 > \bar{P}^2 + \bar{Q}^2 \tag{8}$$

Clearly, if the right-hand side is less than unity, then there are no wrinkles. If it is greater than $(r_i/r_o)^4$, then the entire annulus is wrinkled.

2.3 Wrinkled Region

Since

$$N_\theta = \frac{N_{r\theta}^2}{N_r}$$

we have

$$\frac{d}{d\rho}\left(\rho \bar{N}_r\right) = \frac{\bar{Q}^2}{\left(\rho^4 \bar{N}_r\right)} \tag{9}$$

Integrating gives

$$\bar{N}_r^2 = \frac{1}{\rho^4}\left[\left(\bar{N}_{r_0}^2 + \bar{Q}^2\right)\rho^2 - \bar{Q}^2\right] \tag{10}$$

where $\bar{N}_{r_0}$ is the radial stress resultant at the center plug.

The third of Eq. (1) is nondimensionalized to give

$$\frac{d\bar{w}}{d\rho} = \rho - \frac{\rho^2 + \bar{P}}{\rho \bar{N}_r} \tag{11}$$

where

$$\bar{w} = \left(\frac{a}{r_o}\right)^2 \frac{w}{a}$$

Substituting for $\bar{N}_r$ from Eq. (10) and integrating gives

$$\bar{w} = \bar{w}_0 + \frac{\rho^2 - 1}{2} - \frac{\sqrt{\left(\bar{N}_{r_0}^2 + \bar{Q}^2\right)\rho^2 - \bar{Q}^2}}{3\left(\bar{N}_{r_0}^2 + \bar{Q}^2\right)^{3/2}}$$

$$\times \left[\left(\bar{N}_{r_0}^2 + \bar{Q}^2\right)\rho^2 + 3\bar{N}_{r_0}^2\,\bar{P} + (2 + 3\bar{P})\bar{Q}^2\right] + \frac{\bar{N}_{r_0}}{3\left(\bar{N}_{r_0}^2 + \bar{Q}^2\right)^{3/2}}$$

$$\times \left[(1 + 3\bar{P})\bar{N}_{r_0}^2 + (3 + 3\bar{P})\bar{Q}^2\right] \qquad (12)$$

where $\bar{w}_0$ is the vertical displacement of the central plug.

The first two of Eqs.(2) in dimensionless form are

$$\left.\begin{aligned} \bar{\varepsilon}_r &= \frac{d\bar{u}}{d\rho} + \bar{w} + \frac{1}{2}\left(\frac{d\bar{w}}{d\rho}\right)^2 \\ \bar{\varepsilon}_\theta &= \frac{\bar{u}}{\rho} + \bar{w} \end{aligned}\right\} \qquad (13)$$

where

$$\bar{u} = \left(\frac{a}{r_o}\right)^2 \frac{u}{r_o}$$

and

$$\bar{\varepsilon}_{r,\theta} = \left(\frac{a}{r_o}\right)^2 \varepsilon_{r,\theta}$$

As previously mentioned, the stress and strain relations must be related in a wrinkled region by

$$\bar{\varepsilon}_\theta \bar{N}_\theta = \bar{\varepsilon}_r \bar{N}_r$$

Substituting and multiplying by an integrating factor gives

$$\frac{d}{d\rho}\left(\frac{\bar{u}}{\rho \bar{N}_r}\right) = -\bar{w}\frac{d}{d\rho}\left(\frac{1}{\bar{N}_r}\right) - \frac{1}{2\rho \bar{N}_r}\left(\frac{d\bar{w}}{d\rho}\right)^2$$

$$= -\frac{d}{d\rho}\left(\frac{\bar{w}}{\bar{N}_r}\right) + \frac{1}{\bar{N}_r}\frac{d\bar{w}}{d\rho} - \frac{1}{2\rho \bar{N}_r}\left(\frac{d\bar{w}}{d\rho}\right)^2$$

This can be expressed as

$$\frac{d}{d\rho}\left(\frac{\bar{\varepsilon}_\theta}{\bar{N}_r}\right) = \frac{1}{\bar{N}_r}\frac{d\bar{w}}{d\rho} - \frac{1}{2\rho \bar{N}_r}\left(\frac{d\bar{w}}{d\rho}\right)^2$$

Substituting from Eq. (11) gives

$$\frac{d}{d\rho}\left(\frac{\bar{\epsilon}_0}{\bar{N}_r}\right) = \frac{\rho}{2\bar{N}_r}\left[1 - \frac{(\rho^2 + \bar{P})^2}{\rho^4 \bar{N}_r^2}\right] \tag{14}$$

Going back to Eq. (13) gives

$$\bar{\epsilon}_r = \frac{d}{d\rho}(\rho\bar{\epsilon}_\theta) - \rho\frac{d\bar{w}}{d\rho} + \frac{1}{2}\left(\frac{d\bar{w}}{d\rho}\right)^2$$

$$= \frac{\bar{\epsilon}_\theta}{\bar{N}_r}\frac{d}{d\rho}(\rho\bar{N}_r)$$

In order that one of the principal strains be zero, the shear strain must be related to the direct strains as follows:

$$\bar{\gamma}_{r\theta}^2 = 4\bar{\epsilon}_r\bar{\epsilon}_\theta$$

Therefore, from the dimensionless form of the third of Eq. (2)

$$\frac{d}{d\rho}\left(\frac{\bar{v}}{\rho}\right) = \frac{2}{\rho}\epsilon_\theta\sqrt{\frac{1}{\bar{N}_r}\frac{d}{d\rho}(\rho\bar{N}_r)}$$

or

$$\frac{d}{d\rho}\left(\frac{\bar{v}}{\rho}\right) = \frac{2\bar{Q}}{\rho^3}\frac{\epsilon_\theta}{\bar{N}_r}$$

in which

$$\bar{v} = \left(\frac{a}{r_o}\right)^2 \frac{v}{r_o} \tag{15}$$

Define

$$\left.\begin{aligned} \bar{N}^2 &= \bar{N}_{r_0}^2 + \bar{Q}^2 \\ \bar{M} &= \frac{\bar{Q}^2}{\bar{N}^2} \end{aligned}\right\} \tag{16}$$

Then

$$\bar{N}_r = \frac{\bar{N}}{\rho^2}\sqrt{\rho^2 - \bar{M}}$$

$$\frac{d}{d\rho}\left(\frac{\epsilon_\theta}{\bar{N}_r}\right) = \frac{\rho^3}{2\bar{N}\sqrt{\rho^2 - \bar{M}}}\left[1 - \frac{(\rho^2 + \bar{P})^2}{\bar{N}^2(\rho^2 - \bar{M})}\right]$$

Integrating gives

$$\frac{\bar{\epsilon}_\theta}{\bar{N}_r} = -\frac{1}{\bar{N}^3}\left\{\bar{N}^2\left[F(\rho_e) - F(\rho)\right] - \left[G(\rho_e) - G(\rho)\right]\right\} \tag{17}$$

where

$$F(\rho) = \frac{1}{3}(\rho^2 - \bar{M})^{3/2} + \bar{M}(\rho^2 - \bar{M})^{1/2}$$

$$G(\rho) = \frac{1}{5}(\rho^2 - \bar{M})^{5/2} + \frac{2\bar{P} + 3\bar{M}}{3}(\rho^2 - \bar{M})^{3/2}$$

$$+ (\bar{P} + \bar{M})(\bar{P} + 3\bar{M})(\rho^2 - \bar{M})^{1/2} - \bar{M}(\bar{P} + \bar{M})^2(\rho^2 - \bar{M})^{-1/2} \tag{18}$$

Note that we have used the boundary condition that the circumferential strain must be zero at the outder edge of the wrinkled region, $\rho = \rho_e$. The circumferential strain must also be equal to zero at the central boundary. Setting $\bar{\varepsilon}_\theta\ (1) = 0$ and solving for $\bar{N}$ gives

$$\bar{N} = \sqrt{\frac{G(\rho_e) - G(1)}{F(\rho_e) - F(1)}} \tag{19a}$$

If the annulus is fully wrinkled then $\rho_e = \rho_1$. Then $\bar{N}$ can be easily calculated as a function of $\bar{M}$ and $\bar{P}$. Eq. (16) can be applied to determine $\bar{Q}$ and $\bar{N}_{r_0}$.

If, on the other hand, the membrane is only partly wrinkled, then continuity of the radial stress resultant at $\rho = \rho_e$ requires that

$$\bar{N} = \frac{\rho_e^2 + \bar{P}}{\sqrt{\rho_e^2 - \bar{M}}} \tag{19b}$$

Setting the two expressions for N equal to each other allows the determination of acceptable combinations of ρ_e, $\bar{M}$, and $\bar{P}$. Then $\bar{N}$ and finally the accompanying values of $\bar{Q}$ and $\bar{N}_{r_0}$ can be determined.

For simplicity, the following analysis applies to pure force and pure torque.

2.4 Pure Load

For $Q = 0$, we set $\bar{N} = \bar{N}_{r_0}$, and $\bar{M} = 0$. The expressions for the various quantities in the wrinkled region become

$$\left.\begin{aligned} \bar{N}_r &= \frac{\bar{N}}{\rho} \\ \bar{w} &= \bar{w}_0 + \frac{\rho^2 - 1}{2} - \frac{\rho^3 - 1}{3\bar{N}} - \frac{\bar{P}}{\bar{N}}(\rho - 1) \\ \bar{\epsilon}_\theta &= -\frac{1}{2\bar{N}^2\rho}\left[\frac{\rho^5 - 1}{5} + (2\bar{P} - \bar{N}^2)\frac{\rho^3 - 1}{3} + \bar{P}^2(\rho - 1)\right] \end{aligned}\right\} \quad (20)$$

At the interface, $\epsilon_\theta = 0$, $\rho = \rho_e$, and

$$\bar{N} = \rho_e + \frac{\bar{P}}{\rho_e} \quad (21)$$

Solivng for $\bar{N}$, substituting into the last of Eq. (20), and solving for $\bar{P}$ gives

$$\bar{P} = \rho_e\sqrt{\frac{2\rho_e^3 + 4\rho_e^2 + 6\rho_e + 3}{5(2\rho_e + 1)}} \quad (22)$$

The deflection w must also be zero at $\rho = \rho_e$. Therefore,

$$\bar{w}_0 = (\rho_e - 1)\left[\frac{\bar{P}}{\bar{N}} + \frac{\rho_e^2 + \rho_e + 1}{3\bar{N}} - \frac{\rho_e + 1}{2}\right] \quad (23)$$

Substituting for $\bar{P}$ from Eq. (21) gives

$$\bar{w}_0 = \frac{(\rho_e - 1)^2}{2}\left(1 - \frac{2}{3}\frac{2\rho_e + 1}{\bar{N}}\right) \tag{24}$$

Equations (22) through (24) enable the determination of the manner in which $\bar{w}_0$ and $\bar{N}$ and the extent of the wrinkled area change as $\bar{P}$ is increased above unity. When the entire surface becomes wrinkled ($\rho_e = \rho$), then the following results are obtained.

$$\bar{P} > \rho_1\sqrt{\frac{2\rho_1^3 + 4\rho_1^2 + 6\rho_1 + 3}{5(2\rho_1 + 1)}}$$

$$\bar{N} = \frac{15\bar{P}^2 + 10\left(\rho_1^2 + \rho_1 + 1\right)\bar{P} + 3\left(\rho_1^4 + \rho_1^3 + \rho_1^2 + \rho + 1\right)}{5(\rho^2 + \rho + 1)} \tag{25}$$

$$\bar{w}_0 = \left(\frac{3\bar{P} + \rho_1^2 + \rho_1 + 1}{3\bar{N}} - \frac{\rho_1 + 1}{2}\right)(\rho_1 - 1) \tag{26}$$

Equations (22) to (26) can also be used for negative values of $\bar{P}$ less than minus one by changing the sign of the right-hand side of Eq. (22).

2.5 Pure Torque

For $\bar{P}$ equal zero, the expressions for F ang G in Eq. (18) become

$$\left.\begin{aligned} F(\rho) &= \frac{\sqrt{\rho^2 - \bar{M}}}{3}\,(\rho^2 + 2\bar{M}) \\ G(\rho) &= \frac{\rho^6 + 2\bar{M}\rho^4 + 8\bar{M}^2\rho^2 - 16\bar{M}^3}{5\sqrt{\rho^2 - \bar{M}}} \end{aligned}\right\} \tag{27}$$

Then, Eq. (19a) becomes

$$\bar{N}^2 = \frac{3}{5}\,\frac{\left(\rho_e^6 + 2\bar{M}\rho_e^4 + 8\bar{M}^2\rho_e^2 - 16\bar{M}^3\right)\sqrt{1 - \bar{M}} - (1 + 2\bar{M} + 8\bar{M} - 16\bar{M}^3)\sqrt{\rho_e^2 - \bar{M}}}{\left(\rho_e^4 + \bar{M}\rho_e^2 - 2\bar{M}^2\right)\sqrt{1 - \bar{M}} - (1 + \bar{M} - 2\bar{M}^2)\sqrt{\rho_e^2 - \bar{M}}} \tag{28}$$

If ρ_e is on the outer edge, the quantity $\bar{N}$ can be calculated as a function of $\bar{M}$. Then $\bar{Q}$ and $\bar{N}_{r_0}$ can be determined from

$$\left.\begin{aligned} \bar{Q} &= \bar{N}\sqrt{\bar{M}} \\ \bar{N}_{r_0} &= \bar{N}\sqrt{1 - \bar{M}} \end{aligned}\right\} \tag{29}$$

For values of $\bar{Q}$ slightly greater than one, the region is only partly wrinkled. Then, using Eq. (19b) and solving for $\bar{M}$ gives

$$\bar{M} = \rho_e^2\left(1 - \frac{\rho_e^2}{\bar{N}^2}\right) \tag{30}$$

Substituting from Eq. (28) yields the allowable combinations of ρ_e and $\bar{M}$ for partial wrinkling presented in Table 1. Also given are the associated values of $\bar{Q}$ and $\bar{N}_{r_0}$ found from Eq. (29)

The torsional motion of the hub is of interest. The angle of rotation is equal to

$$\Omega = \frac{v(r_0)}{r_0}$$

Or, by using Eq. (15)

$$\bar{\Omega} = 2\bar{Q} \int_{\rho_e}^{1} \frac{\varepsilon_\theta}{\rho^3 \bar{N}_r} \, d\rho \tag{31}$$

where, as for the strains,

$$\bar{\Omega} = \left(\frac{a}{r_0}\right)^2 \Omega$$

Substituting from Eq. (17) and judiciously using Eq. (28) and integrating yields

$$\bar{\Omega} = \frac{\bar{Q}}{3\bar{N}^3}\left[-3\bar{N}^2\left(\sqrt{\rho_e^2 - \bar{M}} - \sqrt{1 - \bar{M}}\right) + \frac{\rho_e^4 + 4\bar{M}\rho_e^2 - 8\bar{M}^2}{\sqrt{\rho_e^2 - \bar{M}}}\right. \tag{32}$$

$$\left. \times \quad \bar{\theta}\,\frac{1 + 4\bar{M} - 8\bar{M}^2}{\sqrt{1 - \bar{M}}}\right]$$

The values for $\bar{\Omega}$ for the partly wrinkled case are given in Table 1.

2.6 Numerical Results

The load-displacement relations are shown in Figure 1 for pure load. The partly wrinkled membrane exhibits a softening behavior as the load is increased. When the wrinkling reaches the rim, the resulting fully wrinkled membrane stiffens with the application of increased load.

The same behavior is exhibited for pure torsion as seen from Figure 2. It is interesting to note that, although deflections of the membrane begin when the loading parameter ($\bar{P}$ or $\bar{Q}$) exceeds unity, significant movement starts occurring at a value of about two. This phenomenon is similar to that observed for cylinders in bending and is especially pronounced for the torqued dish.

III. IMPLEMENTATION OF A FINITE ELEMENT ALGORITHM FOR A FLAT MEMBRANE

3.1 Finite Element Algorithm

Stresses and deformations in flat membranes may be described within the context of plane stress theory. For the class of problems under consideration, three regimes of structural behavior are possible. First, the membrane may behave in a fully taut manner, in which both principal stresses are positive. In general, this will occur whenever

$$\varepsilon_1 > 0 \quad \text{and} \quad \varepsilon_2 \geq -\nu\varepsilon_1 \tag{33}$$

where

$$\left.\begin{aligned} \varepsilon_1 &= \frac{1}{2}\left[(\varepsilon_x + \varepsilon_y) + \sqrt{(\varepsilon_x - \varepsilon_y)^2 + \gamma_{xy}^2}\right] \\ \varepsilon_2 &= \frac{1}{2}\left[(\varepsilon_x \quad \varepsilon_y) - \sqrt{(\varepsilon_x - \varepsilon_y)^2 + \gamma_{xy}^2}\right] \end{aligned}\right\} \tag{34}$$

In Eqs. (31) and (32), ε_1 and ε_2 represent the local principal strains which are determined from the load-dependent strains ε_x, ε_y, and γ_{xy}.

In regions where Eqs. (33) hold, the stresses in the membrane may be determined from the well known plane stress elasticity relations.

$$\underset{\sim}{\sigma} = D_T \underset{\sim}{\varepsilon} \tag{35}$$

where

$$\left.\begin{aligned} \underset{\sim}{\sigma} &= (\sigma_x, \sigma_y, \tau_{xy})^T \\ \underset{\sim}{\varepsilon} &= (\varepsilon_x, \varepsilon_y, \gamma_{xy})^T \end{aligned}\right\} \tag{36}$$

and

$$D_T = \frac{E}{1-\nu^2} \begin{bmatrix} 1 & \nu & 0 \\ \nu & 1 & 0 \\ 0 & 0 & (1-\nu)/2 \end{bmatrix} \tag{37}$$

where E and ν are the modulus of elasticity and Poisson's ratio of the membrane material, respectively.

In other regions the membrane may behave in a fully slack manner. In general, this will occur whenever

$$\varepsilon_2 \leq \varepsilon_1 \leq 0. \tag{38}$$

In such regions it is clear that the corresponding elastic principal stresses would both be compressive. However, since the membrane cannot support compressive stresses, the membrane is actually stress-free in such regions. Mathematically, this may be expressed as

$$\underset{\sim}{\sigma} = D_s \underset{\sim}{\varepsilon} \tag{39}$$

where

$$D_s = 0. \tag{40}$$

Finally, it is possible for the membrane to develop wrinkles. In this case the stress state is regarded as uniaxial, with the tensile stress aligned along the direction of the wrinkles. Wrinkled behavior will occur whenever

$$\varepsilon_1 > 0 \quad \text{and} \quad \varepsilon_2 < -\nu\,\varepsilon_1. \tag{41}$$

In such cases, the material supports a tensile stress parallel to the principal direction associated with ε_1, but is stress-free in a direction orthogonal to ε_1. Mathematically, the stresses may be expressed as

$$\underset{\sim}{\sigma} = D_w \underset{\sim}{\varepsilon} \tag{42}$$

where

$$D_w \equiv \frac{E}{4}\begin{bmatrix} 2(1+P) & 0 & Q \\ 0 & 2(1-P) & Q \\ Q & Q & 1 \end{bmatrix} \tag{43}$$

and where

$$P = \frac{(\varepsilon_x - \varepsilon_y)}{(\varepsilon_1 - \varepsilon_2)} \quad ; \quad Q = \frac{\gamma_{xy}}{(\varepsilon_1 - \varepsilon_2)} \tag{44}$$

Further discussion of the description of stress-strain behavior within a wrinkled region, and the Stein-Hedgepeth constitutive model which forms the basis for the formulation presented herein, may be obtained from Ref. 16.

It should be pointed out that the choice of a D_w matrix consistent with the Stein-Hedgepeth wrinkle model may not be unique. There may, in fact, be an infinite number of elasticity matrices capable of producing the correct stress-strain relations in a wrinkled element. However, the matrix of Eqn. (43) provides a bounded and symmetric matrix which has been successfully implemented and tested as reported herein and in Ref. 16.

The stress-strain matrices presented above are strain-dependent and must be updated after each load increment. However, all other aspects of the problem formulation are identical to the approach used to solve any nonlinear stress/deformation problem where load increments and iteration for equilibrium are required. Consequently, the algorithm described above may be installed with relatively little effort in a variety of general purpose finite element computer programs which are capable of nonlinear analysis.

3.2 Computer Implementation on the SAP 7 Code at USC

The algorithm presented in Section 3.1 was installed in the SAP 7 computer code at USC where it now resides among the library of available material behavior for plane stress analysis.

A description of the theoretical approach based on the principle of virtual work which is used to formulate the governing equations in the SAP 7 code, and the programmed methods for solving the resulting nonlinear equations is presented in Appendix A.

Most of the required modifications in the rather large SAP 7 code occurred in the subroutine ELPAL. A listing of the revised ELPAL routine which incorporates the wrinkle algorithm is presented in Appendix B.

A listing of the input data used to generate the numerical results for verification examples 1 and 2 (discussed later) are presented in Appendices C and D.

IV. PURE BENDING OF A STRETCHED RECTANGULAR MEMBRANE (FINITE ELEMENT VERIFICATION EXAMPLE NO. 1)

4.1 Problem Description

As a first example of a partly-wrinkled flat membrane, consider a rectangular membrane which is uniformly pretensioned with normal stress σ_0 in the y-direction and with axial load $P = \sigma_0 th$ in the x-direction, as shown in Fig. 3. Note that h is the length of the sides subjected to force P, and t is the thickness of the membrane. After pretensioning, an in-plane bending moment M is applied along the edges shown. As M is increased, eventually a band of vertical wrinkles of length b forms along the lower edge of the membrane as the normal strain ε_x in this region becomes compressive.

The solution for the stress and displacement fields within the resulting partly-wrinkled membrane is not trival. For example, the extent of the wrinkled region is not related in any simple way to the extent of the compression region within a similarly loaded flat plate.

4.2 Analytical Solution

A complete analysis of the problem just described is presented in Ref. [13]. It is shown in this reference that the extent of the wrinkled region may be determined by

$$\frac{b}{h} = \frac{3M}{Ph} - \frac{1}{2} . \tag{45}$$

Furthermore, the overall moment-curvature relation for the membrane is given by

$$\frac{2M}{Ph} = \begin{cases} \frac{1}{3} \quad \frac{Eth^2}{2P} \kappa & ; \quad \frac{Eth^2}{2P} \kappa \leq 1 \\ 1 - \frac{2}{3} \quad \frac{2P}{Eth^2} \quad \frac{1}{\kappa} & ; \quad \frac{Eth^2}{2P} \kappa > 1 \end{cases} \tag{46}$$

and the stress field within the membrane is given by

$$\frac{\sigma_x}{\sigma_o} = \begin{cases} \frac{2\left(\frac{y}{h} - \frac{b}{h}\right)}{\left(1 - \frac{b}{h}\right)^2} & ; \quad \frac{b}{h} \leq \frac{y}{h} \leq 1 \\ 0 & ; \quad 0 \leq \frac{y}{h} \leq \frac{b}{h} \end{cases} \tag{47}$$

$$\frac{\sigma_y}{\sigma_o} = 1 \tag{48}$$

$$\frac{\tau_{xy}}{\sigma_o} = 0 \tag{49}$$

These analytical results are used to evaluate the accuracy of the numerical solution generated by the finite element model discussed in the next paragraph.

4.3 Finite Element Modeling Assumptions

A finite element model of the problem described above was created using the rectangular grid shown in Fig. 4. The model consists of fifty isoparametric quadrilateral elements, each of which contains four internal integration points at which stresses are determined. Displacements at the four corners and midpoints of each side of each element are also determined. The grid contains a total of 181 of such nodal points. The number of unconstrained degrees of freedom in this model is 362.

The problem shown in Fig. 3 is essentially one of specified loading conditions around the perimeter of the membrane. The specification is not complete, however, since only the resultants P and M of the stress distribution along the left and right edges of the membrane are specified, and not the detailed stress distribution itself. This situation is also unsatisfactory from the numerical modeling viewpoint because the model is not restrained from rigid body motion and, the resulting global stiffness matrix would be singular. Therefore, some external constraints on the displacement of at least two nodes is necessary in order to develop a satisfactory finite elment model. It is important to note that such constraints will generally lead to local deviations in the stress and displacement fields from those predicted by the analytical solution.

After investigating several edge constraints and loading conditions, a model was adopted which consists of the constraints $u_x = 0$ at each of the eleven nodes along the left edge of the membrane, where u_x is the nodal displacement in the x-direction. All nodal points along this

edge are free to move in the y-direction except the node at the center of this edge, which is constrained such that $u_y = 0$.

Along the upper and lower edges of the membrane, the loading conditions used in the finite element model consist of vertical tensile loads applied at each node. The magnitude of these nodal forces is determined such that they are equivalent to a uniform tensile normal stress of σ_o along each edge.

In order to apply the resultant tension force P in the x-direction and bending moment M, the nodes along the right edge of the membrane model were attached to a finite element model of a very stiff beam upon which external forces were applied. The attachment between the membrane and beam models was accomplished by requiring continuity of displacements in the x-direction at each node. However, displacements in the y-direction for nodes belonging to the membrane were not required to be the same as those for nodes belonging to the beam, except at the node in the center of the edge. In addition, nodal forces were applied to the beam in such manner that the resultant force was P and the resultant bending moment was M.

Numerical results were generated by first applying the pretensioning forces. These forces correspond to P along the right edge and σ_o along the upper and lower edges. After the equilibrium configuration of the pretensioned membrane was obtained, a bending moment M was applied in small increments to the stiff beam along the right edge of the membrane. An iterative solution for equilibrium displacements was generally required after each increment of bending moment.

4.4 Comparison of Finite Element and Analytical Results

The qualitative nature of the reults of the finite element simulation are shown in Figs. 5 and 6. Shown in Fig. 5 are the directions of the edge displacements along the right edge of the membrane. (The displacements are not to scale.) This displacement pattern reveals the downward translation and clockwise rigid rotation which are expected for the edge displacements of a cantilevered beam subjected to a pure clockwise bending moment.

Shown in Fig. 6 is a plot of the directions of the principal stresses within every element for the case of an advanced loading state. In this state the applied bending moment is so large that about 75% of the membrane surface is wrinkled. The principal stresses are shown centered on each internal integration point as orthogonally directed line segments. The line segments define the orientation of the principal axes of stress. Wrinkled regions are indicated by a single line segment in a direction parallel to the wrinkles. The length of the arrows is not proportional to the magnitude of the principal stress, and in this sense the figure is not to scale. The results indicate that the principal axes of stress are all aligned along the x and y coordinate axes, as expected.

A comparison of the overall moment-curvature behavior of the membrane, as determined by the finite element model and by Eq. (46) is shown in Fig. 7. Note that the numerical results, even for very large curvatures, are very accurate. In fact, the errors are so small as to be nearly imperceptable at this scale.

Shown in Fig. 8 is a comparison of analytical (Eq.(45)) and numerical results for the wrinkle band width, (b/h). Since this band width is not directly available from the finite element code, it was necessary to estimate the location of the boundary between wrinkled and taut regions by linear extrapolation of numerical results for σ_x. This was accomplished by plotting numerical values for σ_x vs. y (as in Fig. 9), then fitting a curve through these points and extrapolating to $\sigma_x = 0$ in order to identify the corresponding value of $y = b$. Repeating this process for three different stress states corresponding to three different levels of bending moment, the data were obtained for Fig. 8. Again it is seen that the errors in the numerical results are less than two percent.

Shown in Fig. 9 are curves for σ_x vs. y for three different levels of bending moment. The analytical results were generated from Eq. (47), and the numerical results were obtained directly from the SAP 7 output files. Although they are not plotted, the numerical and analytical results for τ_{xy} agreed on the value of zero in every element, and σ_y was observed both numerically and analytically to be σ_0 in every element.

The numerical results shown in Fig. 9 correspond to the σ_x stresses at each internal integration point within the vertical strip of five elements located just left of the center of the membrane model shown in Fig. 4. Results for an element strip along the extreme left or right edges of the membrane vary slightly from the plotted results due to imperfect boundary conditions in the model, as previously discussed.

The accuracy of the numerically determined values for σ_x is again found to be very high at every location except for the special case

when the integration point happened to be located very near the boundary y=b. Since no efforts were made to devise an advanced algorithm for such boundary points, the discrepancy in this special case is not surprising. However, the principal observation from Fig. 9 is that the finite element model is capable of providing very accurate results for the detailed stress distribution within the membrane, at almost every point.

V. PURE ROTATION OF A HUB ATTACHED TO A FLAT STRETCHED MEMBRANE (FINITE ELEMENT VERIFICATION EXAMPLE NO. 2)

5.1 Problem Description

As a second example of a partly-wrinkled flat membrane, consider a rigid circular hub of radius a attached to a flat stretched membrane as shown in Fig. 10. The membrane forms an infinite flat sheet and extends indefinitely in all directions. Let the rigid hub be perfectly bonded to the membrane before pretensioning. After the hub is attached, let the membrane be subjected to a uniform edge tension at infinity, so that the stress state in the membrane far from the hub is isotropic with principal stress σ_0. After pretensioning, the hub is subjected to a pure twisting moment M_t, as shown. For sufficiently large M_t the membrane stress state consists of an exterior taut region and an annular interior region which is wrinkled. The extent of the wrinkled region is measured by the wrinkle radius R.

5.2 Analytical Solution

A detailed analysis of a class of problems very similar to the one just described is contained in Ref. [14]. In particular, from Appendix B, of Ref. [14] in the limiting case of an infinite membrane ($b \to \infty$), the wrinkle radius R corresponding to a prescribed twisting moment M_t is governed by

$$\frac{1}{A} + \frac{1}{B} - \ln\left(\frac{B}{A}\right) - \frac{2}{3} = 0 \qquad (50)$$

where

$$A = \frac{\bar{C}_4}{\bar{M}^2} - 1 \quad ; \quad B = \bar{R}^2 \frac{\bar{C}_4}{\bar{M}^2} - 1 \tag{51}$$

$$\bar{C}_4 = \left[\bar{R} + \sqrt{\bar{R}^2 - \left(\frac{\bar{M}}{\bar{R}}\right)^2}\right]^2 + \left(\frac{\bar{M}}{\bar{R}}\right)^2 \tag{52}$$

and where

$$\bar{M} \equiv \frac{M_t}{2\pi a^2 t \sigma_o} \quad ; \quad \bar{R} \equiv \frac{R}{a} \tag{53}$$

In deriving Eqs. (50) through (53) it was assumed that the value of Poisson's ration for the membrane material is $\nu = \frac{1}{3}$, and that the thickness of the membrane is t.

Furthermore, after correction of a typographical error in Eq. (37) of Ref. [14], the induced angle of twist Φ of the rigid hub is found to be governed by

$$\bar{\phi} = \frac{3\bar{M}}{8}\left[\frac{(1/\bar{R}^2) - 1}{B} + \ln\left(\frac{B}{A}\right) + (1/\bar{R}^2) + \frac{5}{3}\right] \tag{54}$$

where $\bar{\phi} \equiv 2G\phi/\sigma_o$ and G is the shear modulus of the membrane.

The simultaneous solution of Eqs. (50), (51), and (52) requires an iterative numerical approach. However, it can be shown that the response is linear (i.e., no wrinkles occur) for $\bar{M} \leq \sqrt{3/2}$. In this regime, one finds that $\bar{M} = \bar{\phi}$, and R is not meaningful. The onset of wrinkling occurs at $\bar{M} = \sqrt{3/2}$ at which $\bar{R} = 1$. For $\bar{M} > \sqrt{3/2}$, the corresponding nonlinear solutions are presented in Table 2.

Furthermore, the principal stresses in the membrane may be shown to be

$$\frac{\sigma_1}{\sigma_o} = \begin{cases} \dfrac{(\bar{C}_4/\bar{r})}{\bar{C}_4 - (\bar{M}/\bar{r})^2} & ; \quad 1 \leq \bar{r} \leq \bar{R} \\ 1 + (\bar{R}/\bar{r})^2 & ; \quad \bar{R} \leq \bar{r} \end{cases} \tag{55}$$

$$\frac{\sigma_2}{\sigma_o} = \begin{cases} 0 & ; \quad 1 \leq \bar{r} \leq \bar{R} \\ 1 - (\bar{R}/\bar{r})^2 & ; \quad \bar{R} \leq \bar{r} \end{cases} \tag{56}$$

where

$$\bar{r} = r/a \tag{57}$$

and r is the radial distance from the center of the hub.

Also shown in Table 2 are numerical values for

$$k \equiv \frac{16\ \tau_{r\theta}(\bar{r} = 4)}{\sigma_r\ (\bar{r} = 4)} = \frac{\bar{M}}{1 + \frac{\bar{R}}{16}\sqrt{\bar{R}^2 - \frac{M^2}{\bar{R}}}} \tag{58}$$

The values for k are used later in determining an equivalent value of $\bar{M}$ in the finite element model for this problem. After the appropriate $\bar{M}$ has been identified, the analytical values for $\bar{R}$, ϕ, (σ_1/σ_o) and (σ_2/σ_o) are compared with the corresponding results from the finite element model, which is described in the next paragraph.

5.3 Finite Element Modeling Assumptions

The creation of a finite element model for this infinite membrane was accomplished by first imagining the problem as being the superposition of an interior problem and an exterior problem which are pieced together at a common interface. Let the interface be a circle of arbitrarily chosen radius r=4a in Fig. 10. Then the exterior problem (r>4a) contains no wrinkled region and may be solved analytically by simple two-dimensional elasticity theory. The interior region so created (r<4a) is a finite dimensional annulus which contains a wrinkled region.

The appropriate interface conditions at r=4a are continuity of σ_r and $\tau_{r\theta}$, and of displacements u_r and u_θ. The approach employed consisted of applying prescribed σ_r and $\tau_{r\theta}$ along r=4a for both problems. The hub in the interior problem was then regarded as fixed against displacement, as was the outer edge in the exterior problem. The angle of twist in the corresponding composite problem was obtained by adding the angle of rotation between the rim r=4a and fixed hub in the interior problem, and the angle of rotation between the rim r=4a and the fixed boundary at infinity in the exterior problem.

The appropriate values of M_t and σ_o were obtained from the known values of σ_r and $\tau_{r\theta}$ applied at r=4a. This was accomplished for given applied stresses σ_r and $\tau_{r\theta}$ at r=4a (which are sufficiently small that R<4a) by first computing k from Eq. (58). For a given value of k, the corresponding value of $\bar{M}$ may be obtained from Table 2 or from Eqs. (50), (51), (52), and (58) by an iterative solution. σ_o may then be found from the equilibrium relation

$$\sigma_o = 16 \frac{\tau_{r\theta}}{\bar{M}} \tag{59}$$

where $\tau_{r\theta}$ is known. Once $\bar{M}$ is determined for a given loading case in the finite element model, M_t is determined as well as σ_o, and the nondimensional stresses and displacements may be compared with the analytical values previously discussed.

The finite element model of the interior problem was created using the quasi-circular grid shown in Fig. 11. The model consists of 36 isoparametric quadrilateral elements, each of which contains four internal integration points at which stresses are determined. Displacements at the four corners and midpoints of each side of each element are also determined. The grid contains a total of 132 of such nodal points. The number of unconstraining degrees of freedom in this model is 264.

The nodes along the hub-membrane interface were considered fixed against displacement. That is, $u_r = u_\theta = 0$ along r=a. Along the outer edge r=4a, σ_r and $\tau_{r\theta}$ are prescribed independently, but are applied such that $\tau_{r\theta}=0$ initially while σ_r is increased to a constant pretension value. After the pretension in σ_r has been achieved, then $\tau_{r\theta}$ is increased in steps. As a result wrinkles are eventually initiated, and the wrinkle radius R increases with increasing $\tau_{r\theta}$.

The principal stresses σ_1 and σ_2 at each integration point within each element are determined by the SAP finite element program, and may be read directly from the output files. The same is true of the nodal displacements u_r and u_θ. The angle of twist ϕ_I for this interior problem may be computed from

$$\phi_I = \frac{u_\theta\ (\bar{r} = 4)}{4a} \qquad (60)$$

where $u_\theta(\bar{r}=4)$ represents the average tangential displacements around the outer perimeter r=4a of the finite element model, as read directly from the computer printout.

The angle of twist ϕ_E for the corresponding exterior problem may be derived from two-dimensional linear elasticity theory. The appropriate boundary conditions for the exterior problem are (1) σ_r and $\tau_{r\theta}$ are prescribed at r=4a (2) σ_r, $\sigma_\theta \to \sigma_o$ and $u_\theta \to 0$ as $r \to \infty$. The solution for ϕ_E may be obtained as

$$\bar{\phi}_E = \frac{2G\phi_E}{\sigma_o} = \frac{\bar{M}}{16}. \tag{61}$$

The total angle of twist for the numerical model is then defined as

$$\phi = \phi_E + \phi_I \tag{62}$$

5.4 Comparison of Finite Element and Analytical Results

The qualitative nature of the numerical results for the interior problem are shown in Fig. 12. The directions of nodal displacements (not to scale) are shown for a typical one-quarter sector of the annular interior region. The displacements are seen to be primarily clockwise rotation, with a inward radial component noticeable near the hub.

Shown in Fig. 13 is a comparison of analytical (eq. (55)) and numerical values for the maximum principal stress (σ_a/σ_o) as a function of radial position (r/a) for four different load cases. The numerical values for σ_1 were obtained directly from the SAP 7 output files for a typical group of these elements which form a sector of the grid in this axisymmetric problem.

The accuracy of the numerically determined values of σ_1 is seen to be very high in all cases.

A comparison of analytical (Eq. (56)) and numerical values for the minimum principal stress (σ_2/σ_0) as a function of radial position (r/a) is shown in Fig. 14, for four different load cases. Again the numerical values for σ_2 were read directly from the SAP 7 output files for elements in a typical sector of the grid. The accuracy of these minimum principal stresses is seen to be considerably less than that of the maximum principal stresses shown in Fig. 13, but nevertheless the numerical values may still be quite adequate for many engineering purposes.

Shown in Fig. 15 is a comparison of the analytical (Eq. (50)) and numerical values for the wrinkle radius (R/a) as a function of the applied torque $\overline{M}$. Since R is not directly available from the SAP 7 output files, it was necessary to estimate R by curve fitting the results for (σ_2/σ_0) vs. (R/a), and then extrapolating to the case (σ_2/σ_0) = 0. This process was repeated for each load case to obtain the data plotted as numerical values in Fig. 15. The accuracy of the numerical values so obtained is found to be adequate for many engineering purposes.

A comparison of the analytical (Eq. (54)) and numerical values for the overall angle of twist $\overline{\phi}$ as a function of the total applied torque $\overline{M}$ is shown in Fig. 16. The numerical values for $\overline{\phi}$ were obtained from Eqs. (60), (61), and (62) as previously described. As shown in the figure, the finite element model produces results of acceptable accuracy for small torques, but the errors increase as the torque levels increase to a maximum of about five percent at $\overline{M} = 5$. As expected, the errors indicate that the finite element model, which in this example involves only three elements in the radial direction, is too stiff in an overall sense. It is expected that a

finite element model with more elements would result in more flexible behavior, and a reduced error in Fig. 16.

VI. ACKNOWLEDGEMENTS

This research was supported in part by Grant No. NAG-1-235 from the National Aeronautics and Space Administration.

VII. REFERENCES

1. Wagner, H., "Flat Sheet Metal Girders with Very Thin Metal Web", Z. Flugtechn. Motorluftschiffahrt, Vol. 20, 1929, Nos. 8, 9, 10, 11, 12 (translation into English, NACA TM 604-606).

2. Reissner E., "On Tension Field Theory", Proc. V Intl. Cong. Appl. Mech., 1938, pp. 88-92

3. Kondo, K., "The General Solution of the Flat Tension Field", J. Soc. Aero. Sci. Nippon, Vol. 5, 1938, p. 41 (in Japanese).

4. Iai, T., "Method of Solution by Means of the Theorem of Maximum Strain Energy of the Problems of Elasticity", J. Soc. Aero. Sci. Nippon. Vol. 10, 1943, p. 96 (in Japanese).

5. Kondo, K. Iai, T., Moriguti, S., and Murasaki, T., Memoirs of the Unifying Study of the Basic Problems in Engineering Sciences by Means of Geometry, Vol. I. (ed. K. Kondo), pp. 417-441. Tokyo: Gakujutsu Bunken Fukyu-Kai.

6. Mansfield, E. H., "Tension Field Theory--A New Approach Which Shows Its Duality With Inextensional Theory", Proc. XII Intl. Cong. Appl. Mech., 1968, pp. 305-320.

7. Mansfield, E. H., "Load Transfer via a Wrinkled Membrane", Proc. Roy. Soc. Lond., Series A, Vol. 316, 1970, pp. 269-289.

8. Mansfield, E. H., "Analysis of Wrinkled Membranes with Anisotropic and Nonlinear Elastic Properties", Proc. Roy. Soc. Lond., Series A. Vol. 353, 1977, pp. 477-498.

9. Mansfield, E. H., "Gravity-Induced Wrinkle Lines in Vertical Membranes", Proc. Royl. Soc. Lond., Series A, Vol. 375, 1981, pp. 307-325.

10. Danielson, D. A., and Natarajan, S., "Tension Field Theory and the Stresses in Stretched Skin", J. Biomechanics, Vol. 8, 1975, p. 135.

11. Wu, C. H., "Sutures in Stretched Membranes, " Q. Appl. Math., April 1980, p. 109.

12. Wu, C. H., and Canfield, T. R., "Wrinkling in Finite Plane-Stress Theory," Q. Appl. Math., July 1981, p. 179.

13. Stein, M., and Hedgepeth, J. M., "Analysis of Partly Wrinkled Membranes", NASA TN D-813, July 1961.

14. Mikulas, M. M., Jr., "Behavior of a Flat Stretched Membrane Wrinkled by the Rotation of an Attached Hub". NASA TN D-2456, 1964.

15. McComb, H. G., Zender, G. W., and Mikulas, M. M., Jr., "The Membrane Approach to Bending Instability of Pressurized Cylindrical Shells", NASA TN D-1510, 1962.

16. Miller, R. K., and Hedgepeth, J. M., "An Algorithm for Finite Element Analysis of Partly Wrinkled Membranes," AIAA J., Vol. 20, pp. 1761-1763 (1982).

17. Taylor, G. I., "On the Shapes of Parachutes" The Scientific Papers of Sir Geoffrey Ingram Taylor, Vol. III, 1963.

18. Houtz, N. E., "Optimization of Inflatable Drag Devices by Isotensoid Design", AIAA Paper 64-437, 1964.

19. Mikulas, M. M., Jr., and Bohon, H. L., "Development Status of Attached Inflatable Decelerators", J. Spacecraft Rock., Vol. 6, No. 4, 1969, pp. 659-660.

20. Mikulas, M. M., Jr., "Behavior of Doubly Curved Partly Wrinkled Membrane Structures Formed From an Initially Flat Membrane", Ph.D. Thesis, Virginia Polytechnic Institute, Blacksburg, Va., 1970.

21. Rossettos, J. N., "Nonlinear Membrane Solutions for Symmetrically Loaded Deep Membranes of Revolution", NASA TN D-3297, 1966.

22. Sanders, J. L., Jr., "Nonlinear Theories for Thin Shells," Q. Appl. Math., Vol. 21, No. 1, 1963., pp. 21-36.

23. Zak, M., "On the Loss of Stability of the Shape of an Ideally Flexible String", PMM Vol. 32, No. 6, 1968, pp. 1092-1096.

24. Zak, M., "Uniqueness and Stability of the Solution of the Small Perturbation Problems of a Flexible Filament with a Free End, PMM Vol. 39, No. 6, 1970, pp. 1048-1052.

25. Zak, M., Non-Classical Problems in Continuum Mechanics, Monograph, 1974, Leningrad (in Russian).

26. Zak, M., "New Aspects in Mechanics of Continuos Media," Rome University, Report No. 11-208, 1977.

27. Zak, M., "Dynamics of Film", J. Elast., Vol. 9, 1979, pp. 171-185.

28. Zak, M., "Snaps in Structures", Shock Vib. Bull., Vol. 49, Pt. 1, 1979, pp. 83-87.

29. Zak, M., "Anisotropic Model of a Membrane", Proc. ASCE Eng. Mech. Div., Spec. Conf., 3rd., Univ. of Texas, Austin, Sept. 17-19, 1979, Publ. by ASCE, 1979, pp. 24-26.

30. Zak, M., "Nonlinear Phenomena in Films of Solar Arrays", 20th Struct. Dyn. Matl. Conf., St. Louis, Mo. April 4-6, 1979.

TABLE 1. PARAMETER COMBINATION FOR PARTIAL WRINKLING WITH PURE TORQUE

ρ_e	$\bar{M}$	$\bar{N}$	$\bar{Q}$	$\bar{N}_{r0}$	$\bar{\Omega}$
1.0	0.7071	1.4142	1.0000	1.0000	0.0000
1.2	.6320	1.6020	1.2375	0.9718	.0004
1.4	.7548	1.7854	1.5516	.8841	.0057
1.6	.8570	1.9617	1.8161	.7418	.0299
1.8	.9284	2.1310	2.0533	.5703	.0968
2.0	.9681	2.2972	2.2603	.4102	.2325
2.5	.9959	2.7267	2.7211	.1738	.9413
3.0	.9993	3.1818	3.1807	.0839	2.2019
3.5	.9998	3.6522	3.6519	.0456	4.0771
4.0	1.0000	4.1312	4.1311	.0270	6.6473
4.5	1.0000	4.6154	4.6154	.0171	10.0394
5.0	1.0000	5.1031	5.1031	.0113	14.3224
5.5	1.0000	4.4932	5.5932	.0078	19.6060
6.0	1.0000	6.0851	6.0851	.0055	24.9899

TABLE 2

Analytical Solutions for Stresses and Displacements
in the Hub Rotation Example of Figure 10

$\bar{M}$	$\bar{R}$	$\bar{\phi}$	$\bar{C}_4$	k
$\sqrt{3/2}$	1	$\sqrt{3/2}$	3	0.8398
0.8683	1.001	0.8683	3.0040	0.8420
0.8776	1.0050	0.8776	3.0201	0.8510
0.8891	1.0100	0.8892	3.0403	0.8622
0.9816	1.0500	0.9849	3.2090	0.9517
1.0976	1.1000	1.1123	3.4387	1.0637
1.3311	1.2000	1.4019	3.9786	1.2869
1.5656	1.3000	1.7454	4.6529	1.5057
1.7987	1.4000	2.1403	5.4774	1.7152
2.0286	1.5000	2.5753	6.4467	1.9122
2.2545	1.6000	3.0386	7.5455	2.0957
2.4765	1.7000	3.5216	8.7593	2.2656
2.6949	1.8000	4.0190	10.0773	2.4225
2.9101	1.9000	4.5276	11.4924	2.5673
3.1226	2.0000	5.0455	13.0000	2.7007
3.5409	2.2000	6.1045	16.2792	2.9355
3.9523	2.4000	7.1901	19.9002	3.1321
4.3585	2.6000	8.2993	23.8547	3.2945
4.7607	2.8000	9.4301	28.1382	3.4266
5.1597	3.0000	10.5810	32.7482	3.5319
5.5563	3.2000	11.7507	37.6829	3.6137
5.9510	3.4000	12.9385	42.9412	3.6748
6.3440	3.6000	14.1432	48.5223	3.7179
6.7356	3.8000	15.3642	54.4256	3.7456
7.1262	4.0000	16.6007	60.6508	3.7599
8.2929	4.5000	20.3968	81.2545	--
9.0677	5.0000	22.9943	96.5952	--
10.2268	5.6000	26.9814	122.0112	--
10.9981	6.0000	29.6953	140.5578	--

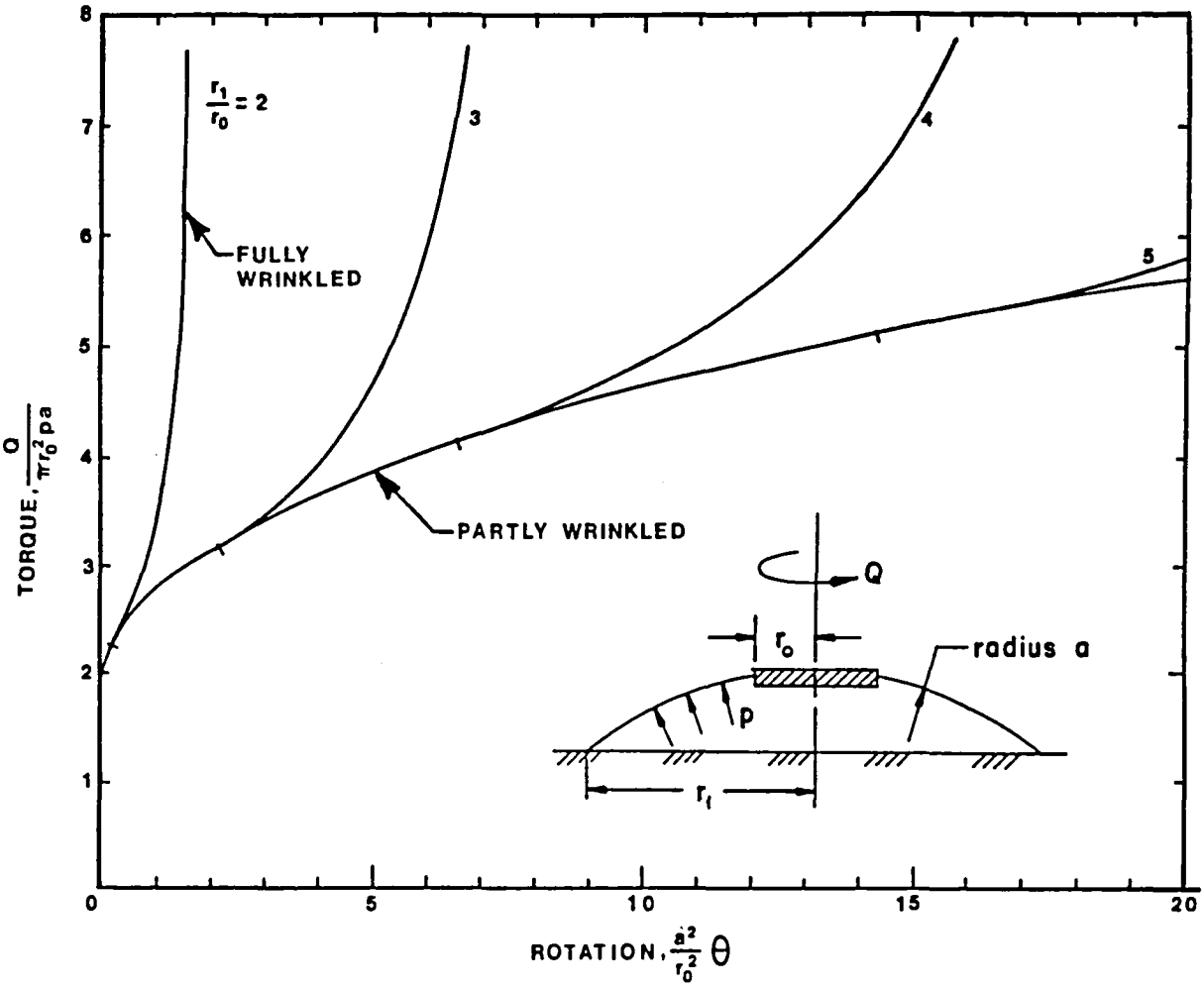

Fig. 1 - Applied Torque vs. Angle of Twist for Axisymmetric Shallow Membrane Problem

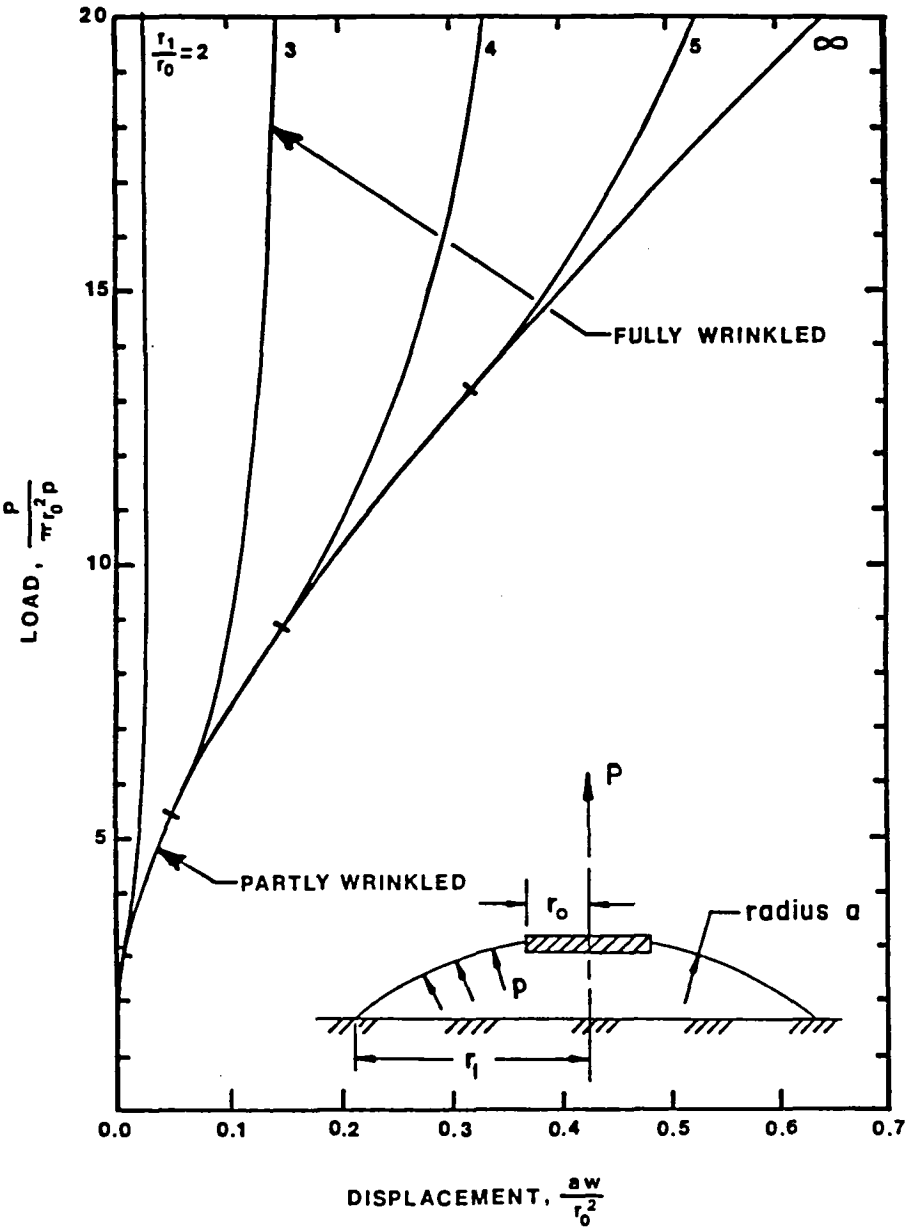

Fig. 2 - Applied Load vs. Vertical Displacement for Axisymmetric Shallow Membrane Problem

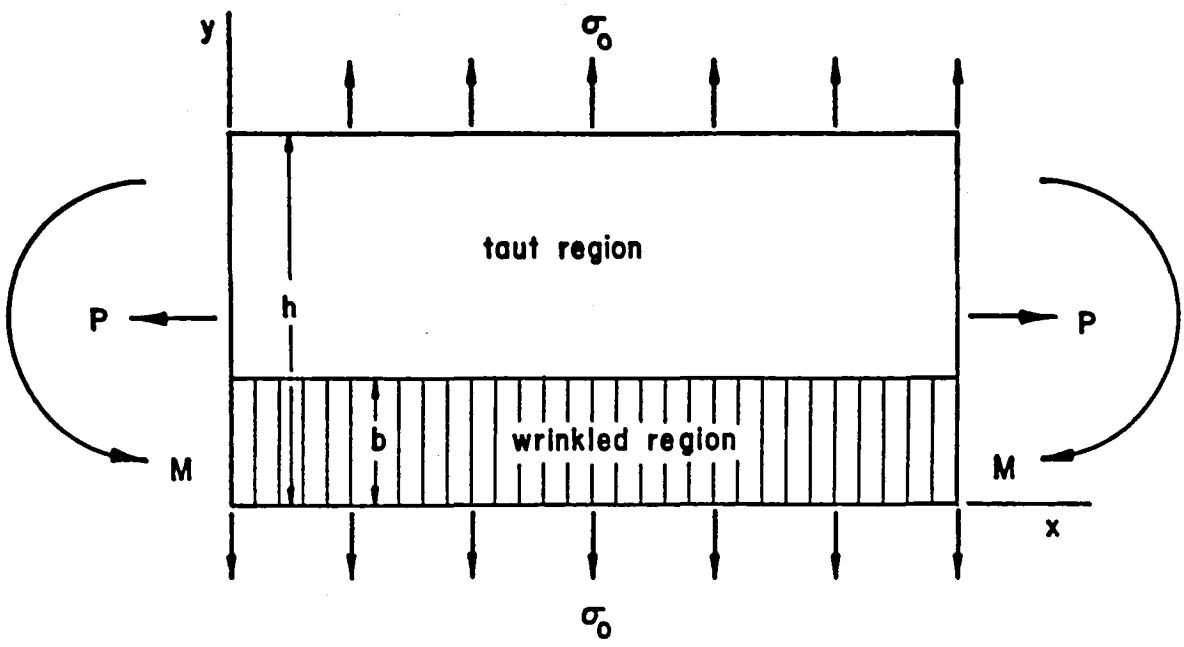

Fig. 3 - Flat Stretched Membrane Subjected to Pure Bending Moment

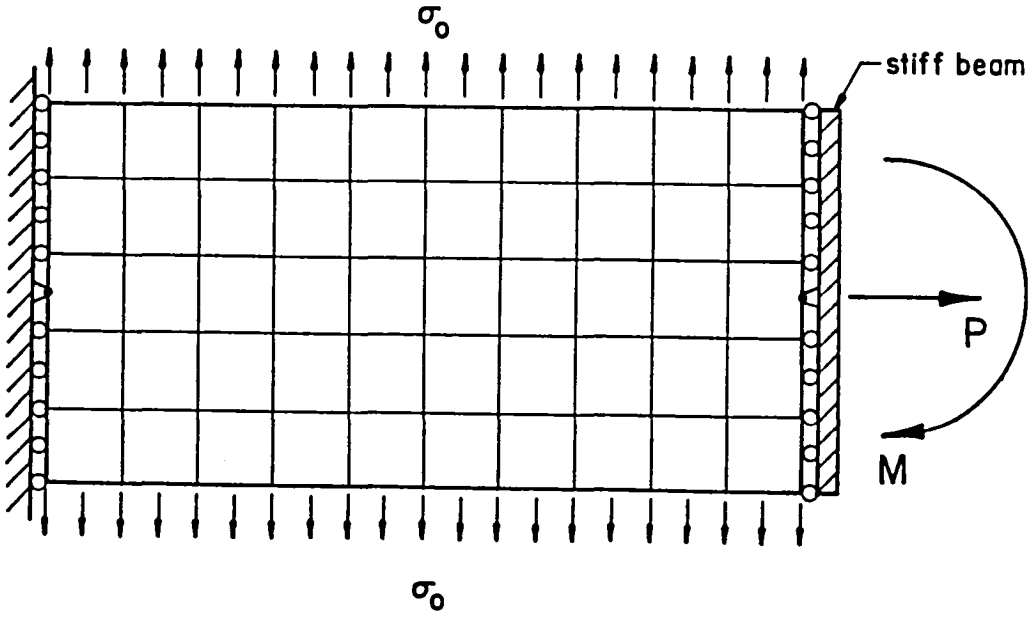

Fig. 4 - Finite Element Model for the Membrane in Fig. 3

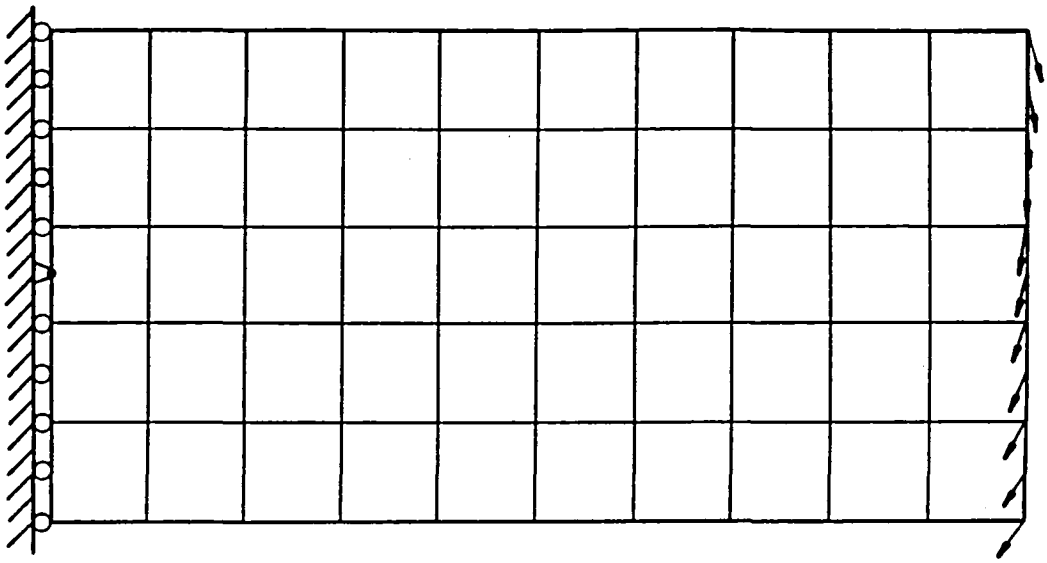

Fig. 5 - Qualitative Plot of Edge Displacements from Numerical Solution for Pure Bending of Rectangular Sheet. (Displacements not to scale.)

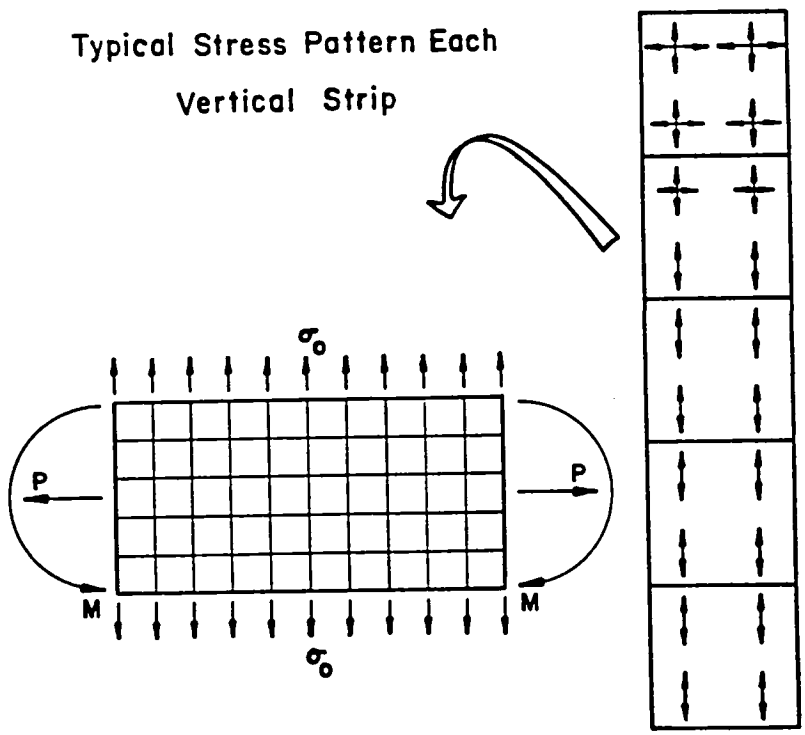

Fig. 6 - Qualitative Plot of Principal Stresses from Numerical Solution for Pure Bending of Rectangular Sheet (Advanced Loading State.)

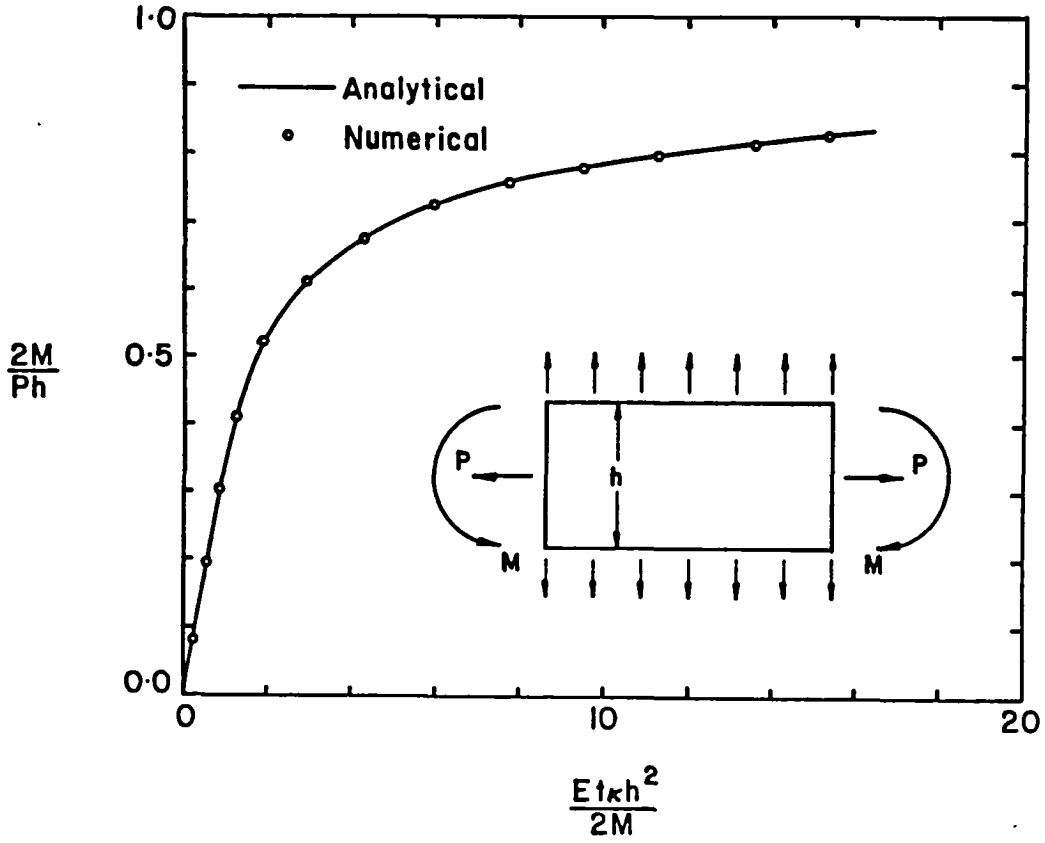

Fig. 7 - Moment-Curvature Relation for Pure Bending of Rectangular Sheet

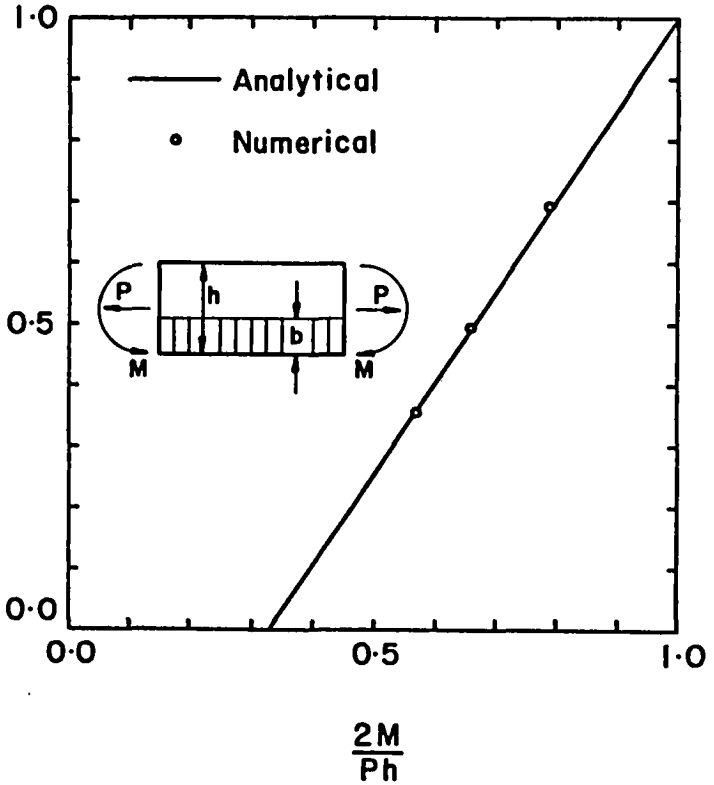

Fig. 8 - Wrinkle Height vs. Bending Moment for Pure Bending of a Rectangular Sheet

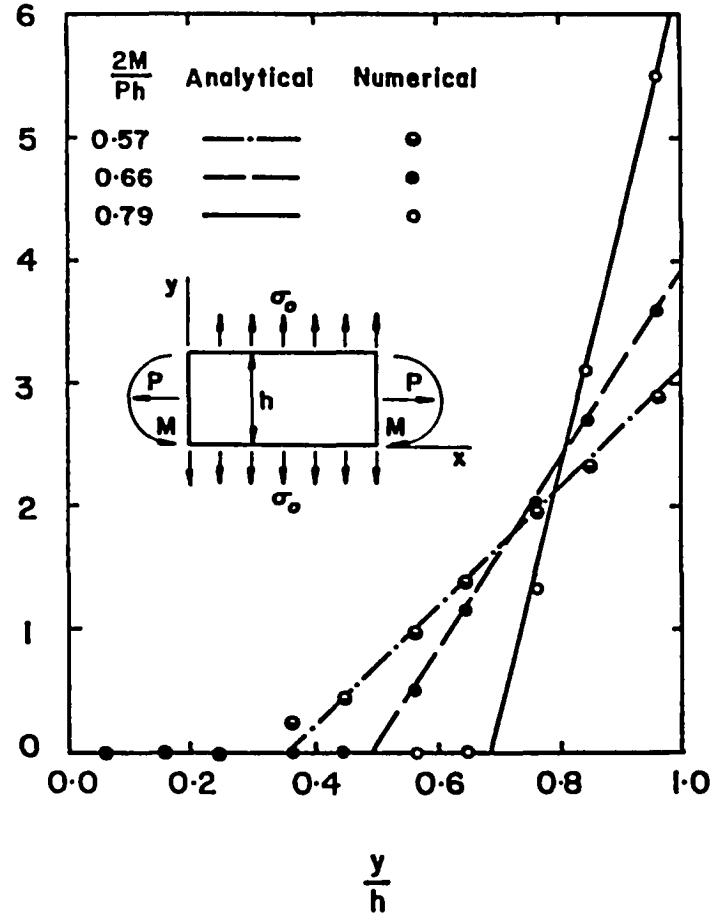

Fig. 9 - Maximum Principal Stress (σ_x) vs. Vertical Position (y) for Pure Bending of a Rectangular Sheet

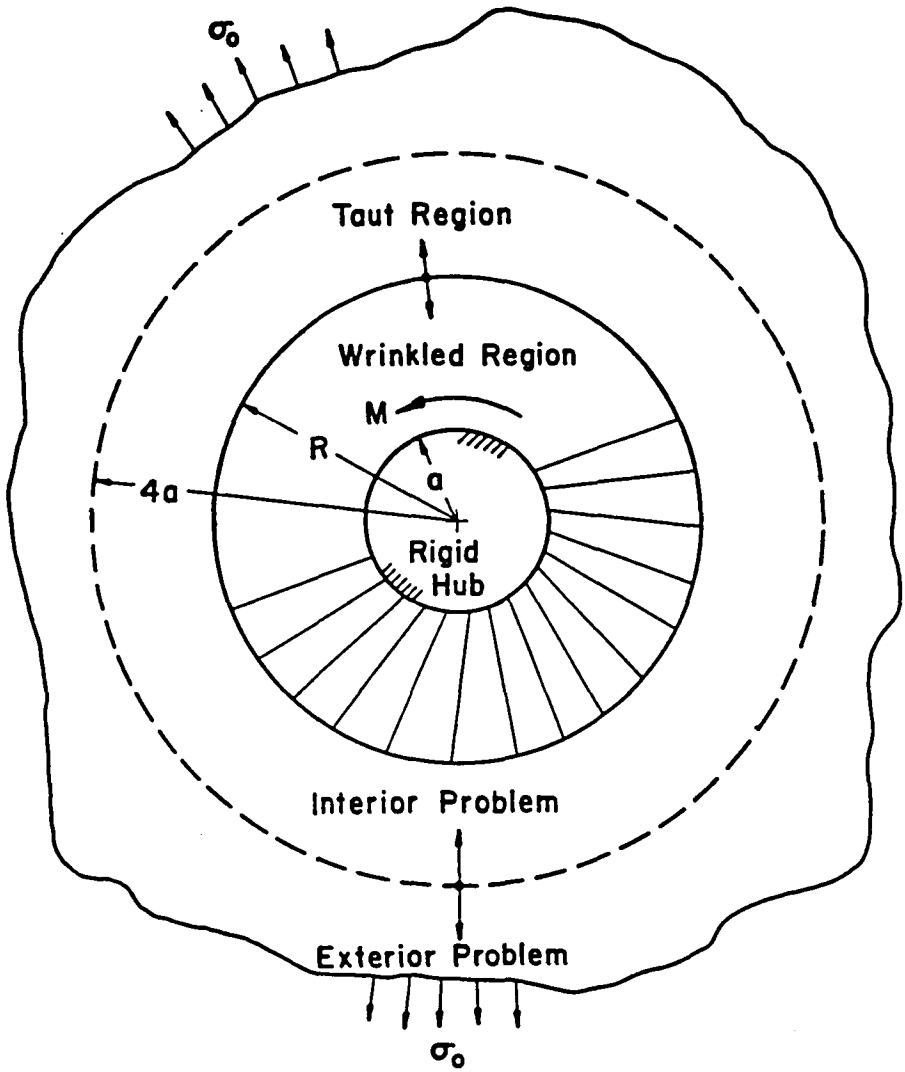

Fig. 10 - Flat Stretched Infinite Membrane Subjected to a Pure Twist M Through an Attached Rigid Hub.

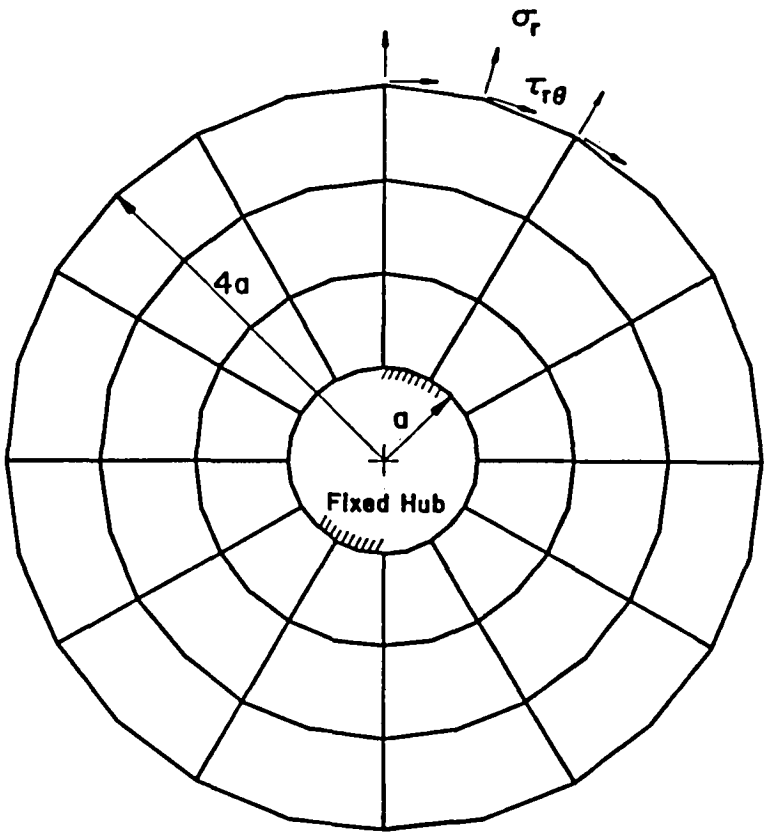

Fig. 11 - Element and Node Configuration for Finite Element Model of Hub Rotation Interior Problem

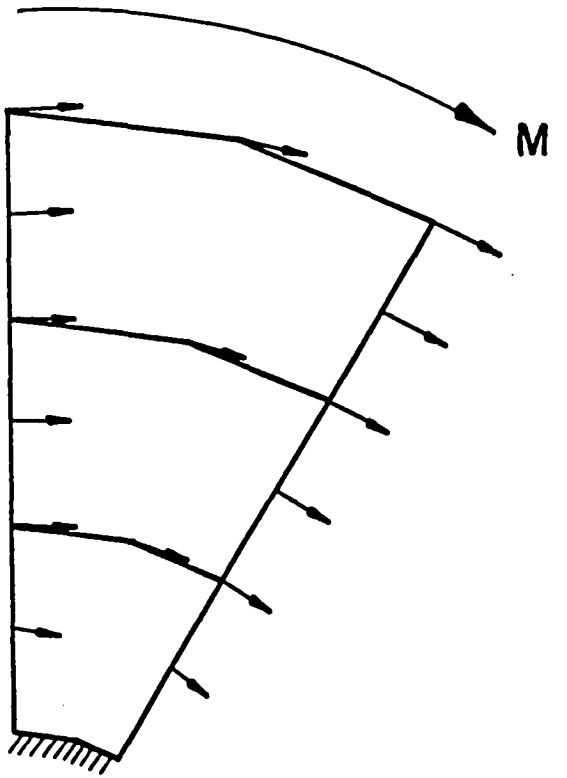

Fig. 12 - Qualitate Nodal Displacements from Numerical Solution of Hub Rotation Interior Problem. (Displacements not to scale.)

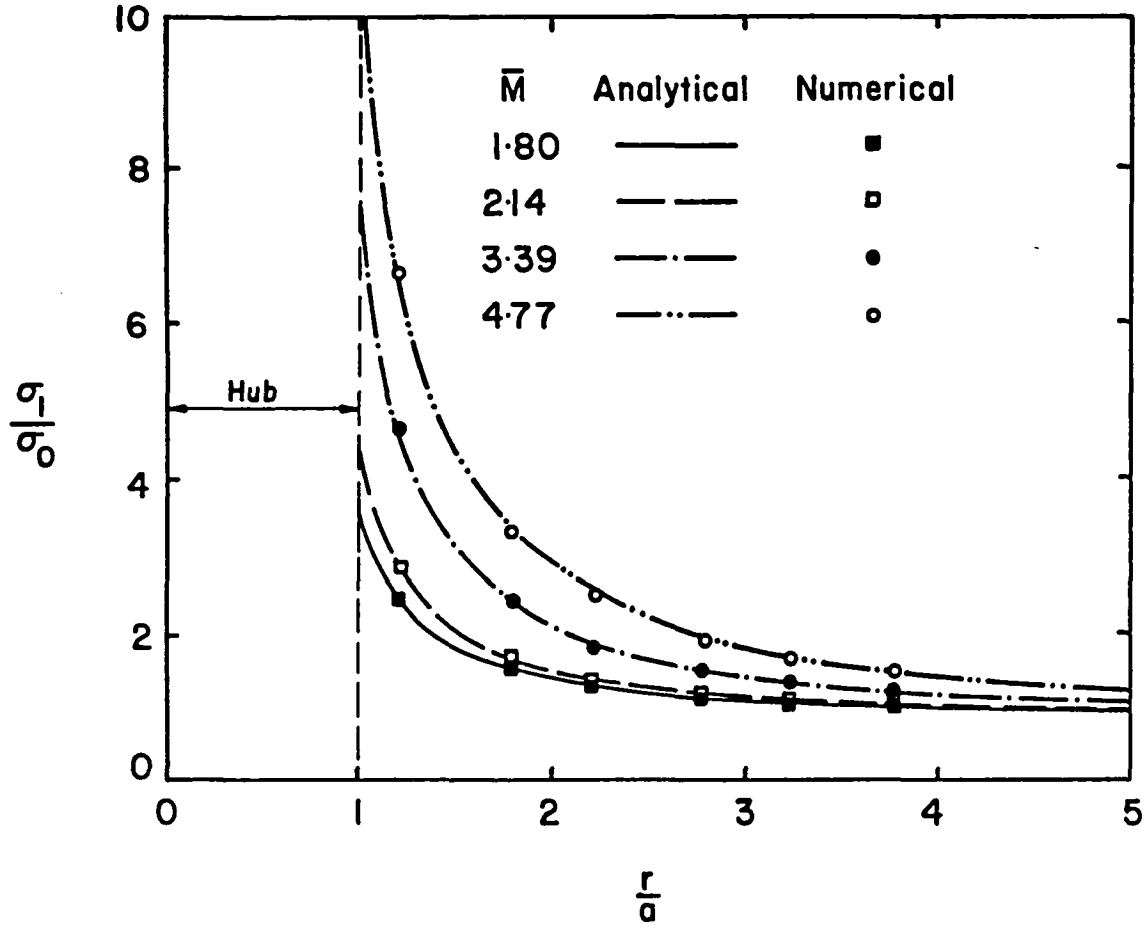

Fig. 13 - Maximum Principal Stress vs. Radial Position for Four Load Cases (Hub Rotation Interior Problem)

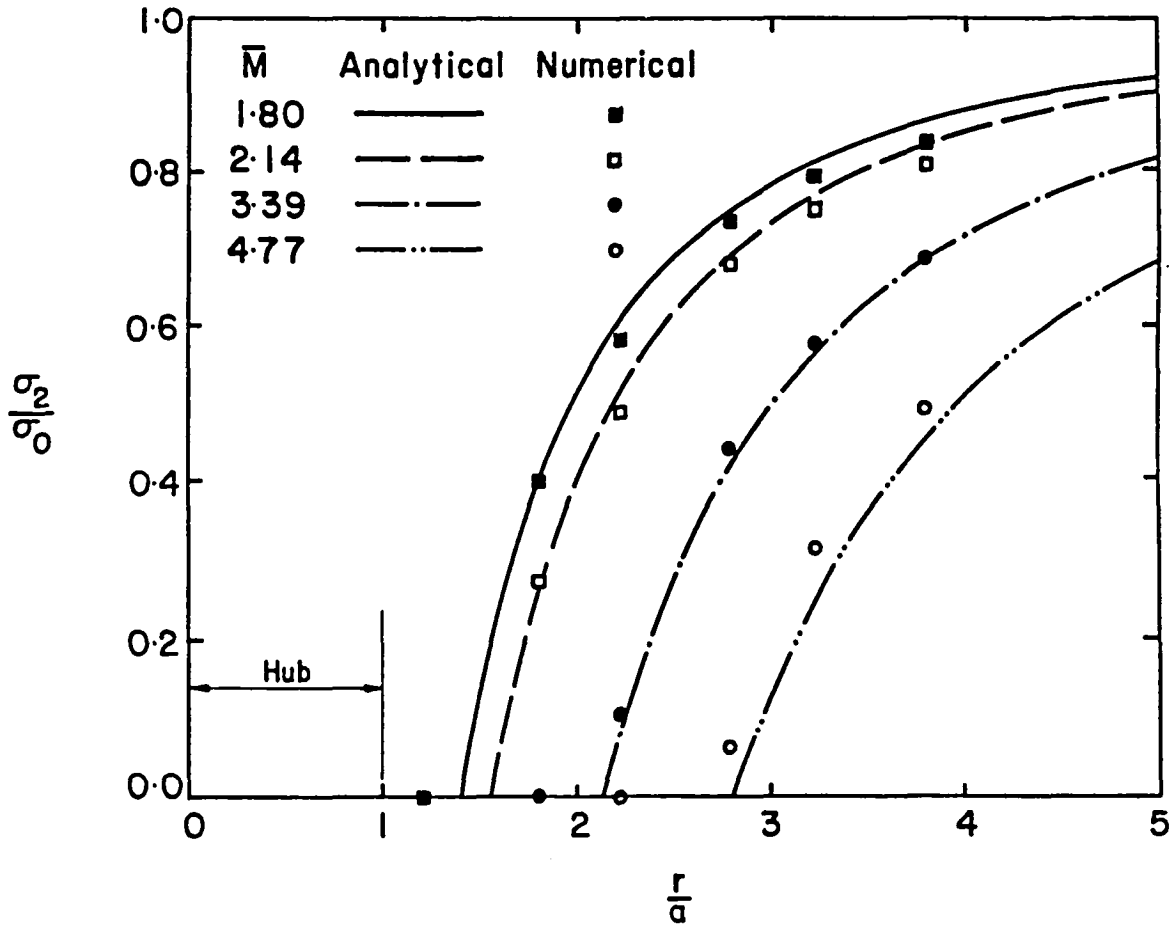

Fig. 14 - Minimum Principal Stress vs. Radial Position for Four Load Cases (Hub Rotation Interior Problem)

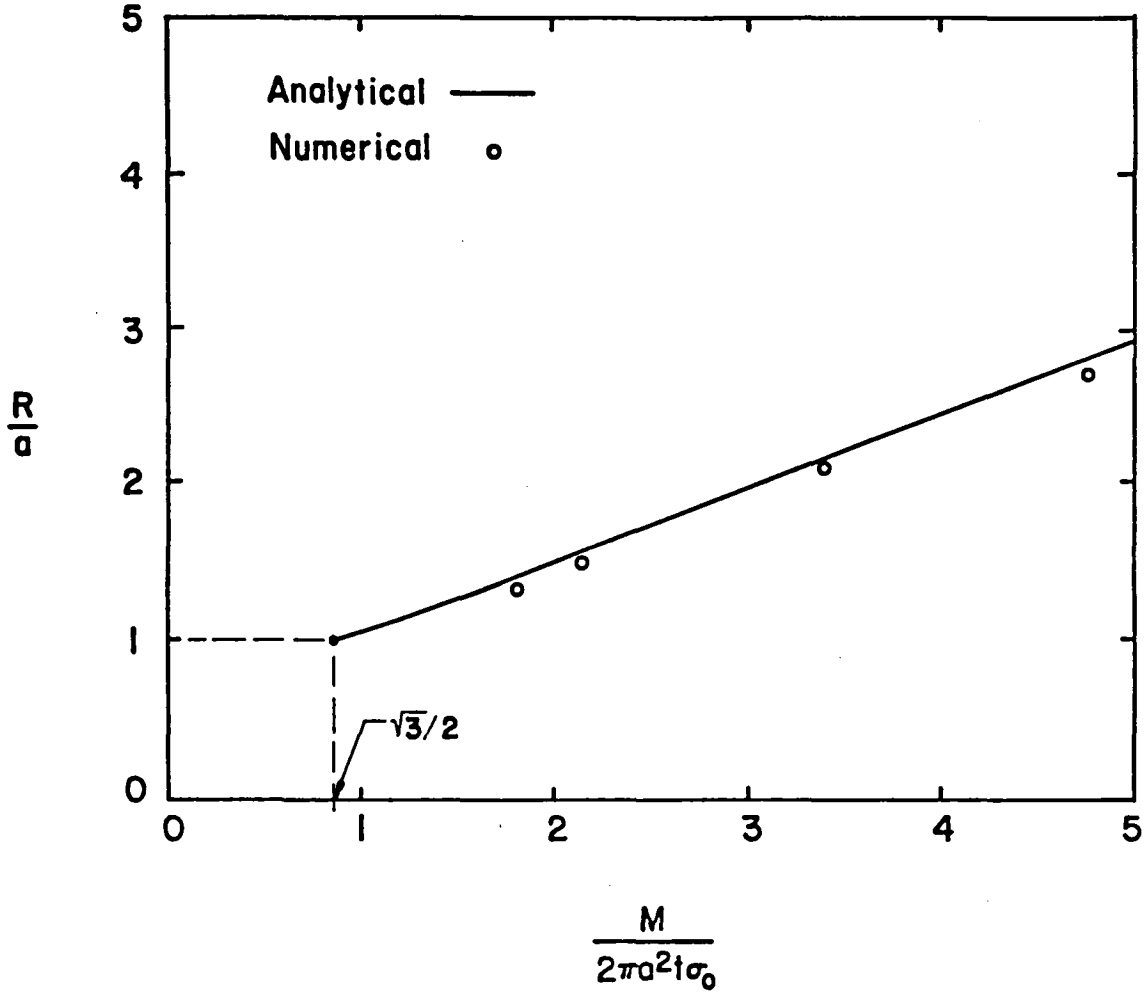

Fig. 15 - Wrinkle Radius R vs. Applied Torque M
for Hub Rotation Interior Problem

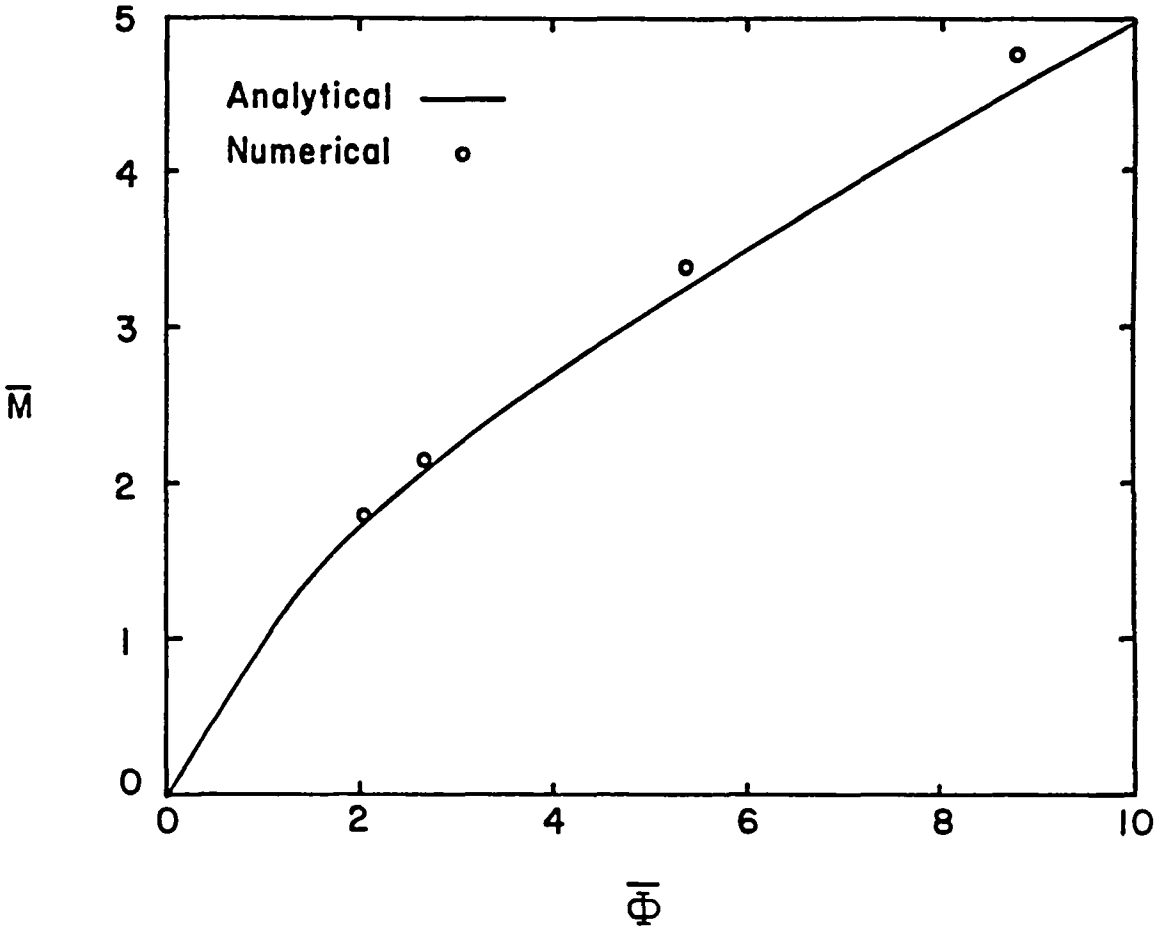

Fig. 16 - Nondimensional Angle of Twist $\bar{\Phi}$ vs. Applied Torque $\bar{M}$ for Hub Rotation Composite Problem

APPENDIX A

FORMULATION AND SOLUTION OF NONLINEAR STRUCTURAL PROBLEMS USING SAP 7

This section will discuss the formulation of the governing equations starting from the principle of virtual displacements and methods for solving the resulting nonlinear equations. The discussion of the formulation of the equations follows references [1] and [2].

FORMULATION

The motion of a general body is shown in Fig. 1. The configuration is known at times 0 and t and the objective is to determine it at time t + Δt. In the following derivation a left superscript indicates the time when the quantity occurs and a left subscript indicates the configuration with respect to which the quantity is measured. In the case of derivatives, a left subscript indicates the time of the coordinate with respect to which the quantity is differentiated. Thus,

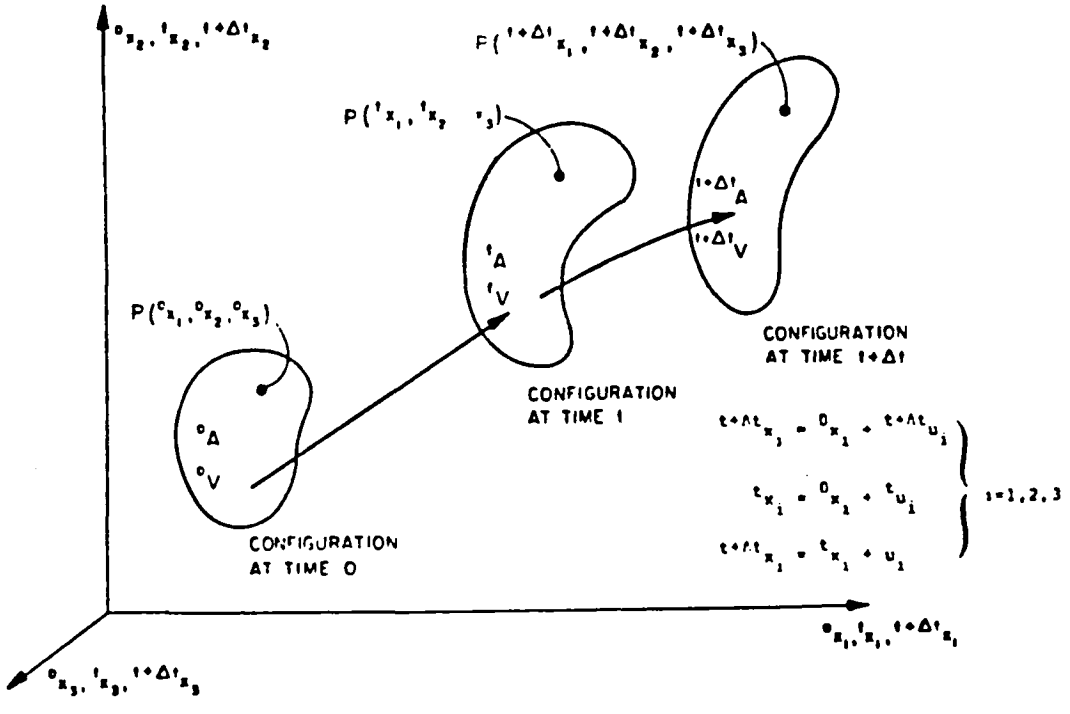

FIG. 1 MOTION OF BODY IN CARTESIAN COORDINATE SYSTEM (FROM REFERENCE (1))

$$ {}^{t+\Delta t}u_{i,j} \equiv \frac{\partial u_i}{\partial ({}^{t+\Delta t}x_j)} \qquad (1) $$

All tensors are referred to Cartesian reference frames. The principle of virtual displacements, written for the current configuration (time = $t+\Delta t$) is

$$ \int_{({}^{t+\Delta t}V)} ({}^{t+\Delta t}\tau_{ij})\, \delta\, ({}_{t+\Delta t}e_{ij})\, ({}^{t+\Delta t}dV) = {}^{t+\Delta t}R $$

where

$$ {}^{t+\Delta t}R = \int_{{}^{o}A} ({}^{t+\Delta t}_{o}t_k)\, \delta u_k\, ({}^{o}dA) + \int_{{}^{o}V} {}^{o}\rho\, ({}^{t+\Delta t}_{o}f_k)\, \delta u_k\, ({}^{o}dV) \qquad (2) $$

The quantities $({}^{t+\Delta t}\tau_{ij})$ are the Cartesian components of the Cauchy (true) stress tensor at time $t+\Delta t$, and $({}^{t+\Delta t}_{o}f_k)$ are surface tractions and body force components at time $t+\Delta t$ but measured with respect to the configuration at time = 0. The variation δu_k is an infinitesimal variation in the current displacement component $({}^{t+\Delta t}u_k)$. The summation convention for repeated indices is used here. The variation in true strain corresponding to the infinitesimal variation in the displacement field is

$$ \delta\, ({}^{t+\Delta t}e_{ij}) = \delta\, \frac{1}{2}\, ({}^{t+\Delta t}u_{i,j} + {}^{t+\Delta t}u_{j,i}) \qquad (3) $$

In dynamic analysis the body force components include inertial effects.

Since the configuration at the current time $t+\Delta t$ is unknown, the principle of virtual displacements, Eq. (1), must be expressed in a form in which all variables are referred to a known state. Then the integration will be performed over known volumes and areas. If the static and kinematic variables are referred to the initial state (time = 0), the formulation is known as Total Lagrangian (TL). If they referred to the previous known state (time = t), the formulation is known as the Updated Lagrangian (UL). The remainder of this derivation will follow the total Lagrangian formulation. References [1] and [2] present details of both the TL and UL formulations.

In the TL formulation the principle of virtual displacements becomes:

$$ \int_{{}^{o}V} ({}^{t+\Delta t}_{o}S_{ij})\, \delta\, ({}^{t+\Delta t}_{o}\epsilon_{ij})\, {}^{o}dV = {}^{t+\Delta t}R \qquad (4) $$

in which ${}^{t+\Delta t}_{o}S_{ij}$ are the components of the 2nd (symmetric) Piola-Kirchoff stress tensor and ${}^{t+\Delta t}_{o}\epsilon_{ij}$ are the components of the Green-Lagrange strain tensor which is written in terms of the current displacements ${}^{t+\Delta t}u_k$:

$$\delta\left({}^{t+\Delta t}_{o}\epsilon_{ij}\right) = \delta\,\frac{1}{2}\left({}^{t+\Delta t}_{o}u_{i,j} + {}^{t+\Delta t}_{o}u_{j,i} + {}^{t+\Delta t}_{o}u_{k,i}\,{}^{t+\Delta t}_{o}u_{k,j}\right) \tag{5}$$

If incremental static and kinematic quantities are defined as

$$\begin{aligned} {}_{o}S_{ij} &\equiv {}^{t+\Delta t}S_{ij} - {}^{t}_{o}S_{ij} \\ {}_{o}\epsilon_{ij} &\equiv {}^{t+\Delta t}_{o}\epsilon_{ij} - {}^{t}_{o}\epsilon_{ij} \\ u_i &\equiv {}^{t+\Delta t}u_i - {}^{t}u_i \end{aligned} \tag{6}$$

the total Green-Lagrange strain increment can be decomposed into linear and nonlinear parts

$${}_{o}\epsilon_{ij} = {}_{o}e_{ij} + {}_{o}\eta_{ij} \tag{7}$$

with

$$\begin{aligned} {}_{o}e_{ij} &= \frac{1}{2}\left[{}_{o}u_{i,j} + {}_{o}u_{j,i} + \left({}^{t}_{o}u_{k,i}\right)\left({}_{o}u_{k,j}\right) + \left({}_{o}u_{k,i}\right)\left({}^{t}_{o}u_{k,j}\right)\right] \\ {}_{o}\eta_{ij} &= \frac{1}{2}\left({}_{o}u_{k,i}\right)\left({}_{o}u_{k,j}\right) \end{aligned} \tag{8}$$

In addition, the increments of 2nd Piola-Kirchoff stress tensor components can be related to the increments of Green-Lagrange strain tensor components by the linear constitutive law

$${}_{o}S_{ij} = {}_{o}C_{ijrs}\left({}_{o}\epsilon_{rs}\right) \tag{9}$$

which is an approximation, since ${}_{o}C_{ijrs}$ changes along the path in the finite increment Δt. Furthermore, the variation in the total strain

$\delta({}^{t+\Delta t}_{o}\epsilon_{ij})$ is equal to the variation in the total strain increment $\delta({}_{o}\epsilon_{ij})$. This equivalence and the relations (6), (7), and (9) can be used to express Eq. (4) in the form

$$\int_{{}^{o}V} {}_{o}C_{ijrs}({}_{o}\epsilon_{rs})\,\delta({}_{o}\epsilon_{ij})\,{}^{o}dV + \int_{{}^{o}V} {}^{t}_{o}S_{ij}\,\delta({}_{o}\eta_{ij})\,{}^{o}dV = {}^{t+\Delta t}R - \int_{{}^{o}V} {}^{t}_{o}S_{ij}\,\delta({}_{o}\epsilon_{ij})\,{}^{o}dV \tag{10}$$

This variational principle represents a nonlinear equation for the incremental displacements u_i. The Updated Lagrangian formulation leads to a completely analogous expression in which the subscripts and superscripts (o) are replaced by (t) and the equivalence of the 2nd Piola-Kirchoff stress tensor ${}^{t}_{t}S_{ij}$ to the Caunchy (true) stress tensor ${}^{t}\tau_{ij}$ is noted. Of course, the constitutive tensor for the U.L. formulation is now ${}_{t}C_{ijrs}$, which takes on different values from ${}_{o}C_{ijrs}$. The relationship between the two constitutive tensors is given by

$${}_{o}C_{mnpq} = \frac{{}^{o}\rho}{{}^{t}\rho}({}^{o}_{t}x_{m,i})({}^{o}_{t}x_{n,j})({}_{t}C_{ijrs})({}^{o}_{t}x_{p,r})({}^{o}_{t}x_{q,s}) \tag{11}$$

$${}_{t}C_{mnpq} = \frac{{}^{t}\rho}{{}^{o}\rho}({}^{t}_{o}x_{m,i})({}^{t}_{o}x_{n,j})({}_{o}C_{ijrs})({}^{t}_{o}x_{p,r})({}^{t}_{o}x_{q,s}) \tag{12}$$

Equation (10) can be transformed into a system of simultaneous nonlinear algebraic equations by division of the volume ${}^{o}V$ into an assemblage of finite elements and use of isoparametric interpolation

$${}^{o}x_i = \sum_{k=1}^{N} h_k({}^{o}x_i^k) \quad ; \quad u_i = \sum_{k=1}^{N} h_k(u_i^k) \tag{13}$$

in each element, where N is the number of nodal points in the isoparametric element and h_k are appropriate interpolation polynomials. Integration is carried out numerically, usually by Gaussian quadrature. Reference [2] first linearized Eq. (10) by replacing ${}_{o}\epsilon_{rs}$ by ${}_{o}e_{rs}$ and $\delta({}_{o}\epsilon_{ij})$ by $\delta({}_{o}e_{ij})$ and then perform modified Newton iterations, setting

$${}^{t+\Delta t}u_i^{(k)} = {}^{t+\Delta t}u_i^{(k-1)} + \Delta u_i^{(k)} \tag{14}$$

in which k is the iteration number and ${}^{t+\Delta t}u_i^{(0)} \equiv {}^{t}u_i$.

As given in Reference [3] the substitution of Eq. (13) into Eq. (10) yield the following matrix equations.

TABLE 1 FINITE ELEMENT MATRICES

ANALYSIS TYPE	INTEGRAL	MATRIX EVALUATION
IN ALL ANALYSES	$\int_{{}^0V} {}^0\rho \; {}^{t+\Delta t}\ddot{u}_k \; \delta u_k \; {}^0dv$	$M \; {}^{t+\Delta t}\ddot{u} = {}^0\rho \left(\int_{{}^0V} H^T \; H \; {}^0dv \right) {}^{t+\Delta t}\ddot{u}$
	${}^{t+\Delta t}R = \int_{{}^0A} {}^{t+\Delta t}_{\;\;0}t_k \; \delta u_k \; {}^0da$	${}^{t+\Delta t}R = \int_{{}^0A} H_S^T \; {}^{t+\Delta t}_{\;\;0}t \; {}^0da$
	$+ \int_{{}^0V} {}^0\rho \; {}^{t+\Delta t}_{\;\;0}f_k \; \delta u_k \; {}^0dv$	$+ {}^0\rho \int_{{}^0V} H^T \; {}^{t+\Delta t}_{\;\;0}f \; {}^0dv$
A. LINEAR ANALYSIS	$\int_{{}^0V} C_{ijrs} \; {}^{t+\Delta t}e_{rs} \; \delta e_{ij} \; {}^0dv$	$K \; {}^{t+\Delta t}u = \left(\int_{{}^0V} B_L^T \; C \; B_L \; {}^0dv \right) {}^{t+\Delta t}u$

TABLE 1 (cont'd)

ANALYSIS TYPE	INTEGRAL	MATRIX EVALUATION
B. MATERIAL NONLINEARITY ONLY	$\int_{0_V} C_{ijrs}\ e_{rs}\ \delta e_{ij}\ {}^{0}dv$	${}^{t}K\ u = \left(\int_{0_V} B_L^T\ C\ B_L\ {}^{0}dv\right) u$
	$\int_{0_V} {}^{t}\sigma_{ij}\ \delta e_{ij}\ {}^{0}dv$	${}^{t}F = \int_{0_V} B_L^T\ {}^{t}\hat{\Sigma}\ {}^{0}dv$
C. TOTAL LAGRANGIAN FORMULATION	$\int_{0_V} {}^{0}C_{ijrs}\ {}^{0}e_{rs}\ \delta_0 e_{ij}\ {}^{0}dv$	${}^{t}_{0}K_L\ u = \left(\int_{0_V} {}^{t}_{0}B_L^T\ {}^{0}C\ {}^{t}_{0}B_L\ {}^{0}dv\right) u$
	$\int_{0_V} {}^{t}_{0}S_{ij}\ \delta_0 \eta_{ij}\ {}^{0}dv$	${}^{t}_{0}K_{NL}\ u = \left(\int_{0_V} {}^{t}_{0}B_{NL}^T\ {}^{t}S\ {}^{t}_{0}B_{NL}\ {}^{0}dv\right) u$
	$\int_{0_V} {}^{t}_{0}S_{ij}\ \delta_0 e_{ij}\ {}^{0}dv$	${}^{t}_{0}F = \int_{0_V} {}^{t}_{0}B_L^T\ {}^{t}\hat{S}\ {}^{0}dv$

TABLE 1 (cont'd)

ANALYSIS TYPE	INTEGRAL	MATRIX EVALUATION
D. UPDATED LAGRANGIAN FORMULATION	$\int_{t_V} {}^tC_{ijrs}\ {}^te_{rs}\ \delta\,{}^te_{ij}\ {}^tdv$	${}^tK_L\ u = \left(\int_{t_V} {}^tB_L^T\ {}^tC\ {}^tB_L\ {}^tdv\right) u$
	$\int_{t_V} {}^t\tau_{ij}\ \delta\,{}^t\eta_{ij}\ {}^tdv$	${}^tK_{NL}\ u = \left(\int_{t_V} {}^tB_{NL}^T\ {}^t\tau\ {}^tB_{NL}\ {}^tdv\right) u$
	$\int_{t_V} {}^t\tau_{ij}\ \delta\,{}^te_{ij}\ {}^tdv$	${}^tF = \int_{t_V} {}^tB_L^T\ {}^t\hat{\tau}\ {}^tdv$

Numerical Time Integration

The incremental equilibrium equations must be solved at each time step using a numerical integration scheme. In SAP7 the Wilson θ - method and Newmark method are used. This section follows the formulation given in Reference [3].

In the Wilson θ - method a linear variation of acceleration is assumed over the time increment $\tau = \theta \Delta t$, where (for unconditional stability in the analysis of linear systems) $\theta \geq 1.37$, and the equilbrium equations are considered at time $t + \tau$,

$$M\ {}^{t+\tau}\ddot{u} + C\ {}^{t+\tau}\dot{u} + {}^{t}K\ u = {}^{t+\tau}R - {}^{t}F \qquad (1)$$

where ${}^{t+\tau}R = {}^{t}R = \theta\ ({}^{t+\Delta t}R - {}^{t}R)$, and u is the change in displacement vector during the time interval t to $t + \tau$, i.e. $u = {}^{t+\tau}u - {}^{t}u$. Using the linear acceleration assumption it follows that

$${}^{t+\tau}\dot{u} = {}^{t}\dot{u} + \frac{\tau}{2}\ ({}^{t+\tau}\ddot{u} + {}^{t}\ddot{u}) \qquad (2)$$

$${}^{t+\tau}u = {}^{t}u + \tau\ {}^{t}\dot{u} + \frac{\tau^2}{6}\ ({}^{t+\tau}\ddot{u} + 2\,{}^{t}\ddot{u}) \qquad (3)$$

which gives

$${}^{t+\tau}\ddot{u} = \frac{6}{\tau^2}\ u - \frac{6}{\tau}\ {}^{t}\dot{u} - 2\,{}^{t}\ddot{u} \qquad (4)$$

and

$${}^{t+\tau}\dot{u} = \frac{3}{\tau}\ u - 2\,{}^{t}\dot{u} - \frac{\tau}{2}\ {}^{t}\ddot{u} \qquad (5)$$

Substituting the relations (4) and (5) into Eq. (1), an equation with u as the only unknown is obtained. Solving for u and using the linear acceleration assumption, the required displacement, velocity and acceleration vectors are obtained,

$$ {}^{t+\Delta t}\ddot{u} = \left(1 - \frac{1}{\theta}\right) {}^{t}\ddot{u} + \frac{1}{\theta} {}^{t+\tau}\ddot{u} \qquad (6) $$

$$ {}^{t+\Delta t}\dot{u} = {}^{t}\dot{u} + \frac{\Delta t}{2} \left({}^{t}\ddot{u} + {}^{t+\Delta t}\ddot{u} \right) \qquad (7) $$

$$ {}^{t+\Delta t}u = {}^{t}u + \Delta t \, {}^{t}\dot{u} + \frac{\Delta t^2}{6} \left({}^{t+\Delta t}\ddot{u} + 2 {}^{t}\ddot{u} \right) \qquad (8) $$

EQUILIBRIUM ITERATION

In order to avoid large integration errors we may choose to iterate in each load step until the equilibrium equations are satisfied within a given tolorence. For a single finite element, in the TL formulation the equation used for iteration is given as,

$$ \left({}^{t}_{0}K_{L} + {}^{t}_{0}K_{NL} \right) \Delta u^{(i)} = {}^{t+\Delta t}R - {}^{t+\Delta t}_{0}F^{(i-1)} - M \, {}^{t+\Delta t}\ddot{u}^{(i)} \qquad (9) $$

$$ i = 1,2,3 \ldots $$

where

$$ {}^{t+\Delta t}u^{(i)} = {}^{t+\Delta t}u^{(i-1)} + \Delta u^{(i)} . $$

A more detailed description of the equilibrium iteration equations can be found in Reference [3].

APPENDIX B

SAP 7 SUBROUTINE ELPAL

```
      SUBROUTINE ELPAL (PROP,SIG,EPS,YIELD,IPEL)
C     IMPLICIT REAL*8(A-H,O-Z)
C.....THIS PROGRAM CAN BE USED IN SINGLE PRECISION ON CDC COMPUTERS
C.    AND DOUBLE PRECISION ON IBM,UNIVAC,DEC VAX 780/11 AND PRIME
C.    COMPUTERS. ACTIVATE,DEACTIVATE OR ADJUST THE ABOVE CARD FOR
C.    SINGLE OR DOUBLE PRECISION ARITHMETIC.
C.....................................................................
C
C. . . . . .
C.
C.      IST     NUMBER OF STRESS COMPONENTS
C.      ISR     NUMBER OF STRAIN COMPONENTS
C.      SIG     STRESSES AT THE END OF THE PREVIOUS UPDATE
C.      EPS     STRAINS  AT THE END OF THE PREVIOUS UPDATE
C.      RATIO   PART OF STRAIN INCREMENT TAKEN ELASTICALLY
C.      DELEPS  INCREMENT IN STRAINS
C.      DELSIG  INCREMENT IN STRESSES, ASSUMING ELASTIC BEHAVIOR
C.
C.      PROP(1) YOUNG S  MODULUS
C.      PROP(2) POISSON S  RATIO
C.      PROP(3) INITIAL YIELD STRESS IN SIMPLE TENSION
C.      PROP(4) STRAIN HARDENING MODULUS
C.
C.      IPEL    = 1, MATERIAL ELASTIC
C.              = 2, MATERIAL PLASTIC
C.
C. . . . . .
C
      COMMON /EL/ IND,ICOUNT,NPAR(20),NUMEG,NEGL,NEGNL,IMASS,IDAMP,ISTA
     1,NODE,KLIN,ISIG,IMASSN,IDAMPN
      COMMON /VAR / NG,KPRI,MODEX,KSTEP,ITE,ITEMAX,IREF,IEQREF,INOCMD
     1,INPCMD
      COMMON /VMISES/ A1,B1,C1,D1,A2,B2,C2,D2,YLD,BM,ISR,IST
      COMMON /MATMOD/ STRESS(4),STRAIN(4),C(4,4),THESTR(4),TEMP,IPT,NEL
      COMMON /DISP3/ DISD(9)
      COMMON /PLOT/TIME,IPLT,IPTEL,IPLTDF,IPLTND(2,8),
     *NUMEL,NPTS,IPS,IPES
      COMMON /IWRINK/JWR
C
      DIMENSION PROP(1),SIG(1),EPS(1)
      DIMENSION TAU(4),DELSIG(4),DELEPS(4),DEPS(4),STATE(2)
C
      EQUIVALENCE (NPAR(3),INDNL),(NPAR(5),ITYP2D),(DELEPS,DEPS)
C
      DATA NGLAST/1000/, STATE/1HE,1HP/
C
      SQRT(Q)=DSQRT(Q)
C.....THIS PROGRAM CAN BE USED IN SINGLE PRECISION ON CDC COMPUTERS
C.    AND DOUBLE PRECISION ON IBM,UNIVAC,DEC VAX 780/11 AND PRIME
C.    COMPUTERS. ACTIVATE,DEACTIVATE OR ADJUST THE ABOVE CARD FOR
C.    SINGLE OR DOUBLE PRECISION ARITHMETIC.
C.....................................................................
C
      IF (IPT.NE.1) GO TO 110
C
      IST=4
```

```
      IF (ITYP2D.EQ.2) IST=3
      ISR=3
      IF (ITYP2D.EQ.0) ISR=4
      YM=PROP(1)
      PV=PROP(2)
      D1=PV/(PV - 1.0D0)
      A2=YM/(1.0D0+PV)
      B2=(1.0D0-PV)/(1.0D0-2.0D0*PV)
      C2=PV/(1.0D0-2.0D0*PV)
      D2=YM*PROP(4)/(YM-PROP(4))
      C1=A2/2.0D0
      BM=YM/(1.0D0          - 2.0D0*PV)/3.0D0
C
      IF (ITYP2D.EQ.2) GO TO 105
C
C     PLANE STRAIN  /  AXISYMMETRIC
      B1=A2*C2
      A1=B1+A2
      GO TO 110
C
C     PLANE STRESS
105   A1=YM/(1.D0-PV*PV)
      B1=A1*PV
C
110   YLD = YIELD
C
C
C        1. CALCULATE INCREMENTAL STRAINS
C
      DO 120 I=1,ISR
120   DELEPS(I) = STRAIN(I) - EPS(I)
C
C
C     CHECK FOR WRINKLING BEHAVIOR
C
C   aaaaaaaaaaaaaaaaaaaaaaaaaaaaaaaaaaaaaaaaaaaaaaaaaa
C
      JP=1
C
      IF(JWR.EQ.0)GO TO 30
      EBS=1.E-9
      A=STRAIN(1)+STRAIN(2)
      B=STRAIN(1)-STRAIN(2)
      E12=STRAIN(3)
      E=E12*E12
      E1=(A+SQRT(B*B+E))/2
      E2=(A-SQRT(B*B+E))/2
      IF(E1)24,20,20
 24   JP=2
      DO 25 I=1,4
        SIG(I)=0.D0
 25   DELSIG(I)=0.0D0
      GO TO 150
 20   EP=PV*E1+E2
      IF(EP+EBS)26,30,30
 26   JP=3
      P=B/(E1-E2)
      Q=E12/(E1-E2)
      P1=(1+P)*YM/2.D0
      P2=(1-P)*YM/2.D0
      Q1=Q*YM/4.D0
```

```
      Q2=YM/4
      DELSIG(1)=P1*DELEPS(1)+Q1*DELEPS(3)
        SIG(1)=P1*EPS(1)+Q1*EPS(3)
      DELSIG(2)=P2*DELEPS(2)+Q1*DELEPS(3)
        SIG(2)=P2*EPS(2)+Q1*EPS(3)
      DELSIG(3)=Q1*(DELEPS(1)+DELEPS(2))+Q2*DELEPS(3)
        SIG(3)=Q1*(EPS(1)+EPS(2))+Q2*EPS(3)
      DELSIG(4)=0.0D0
        SIG(4)=0.0D0
      GO TO 150
C
C   @@@@@@@@@@@@@@@@@@@@@@@@@@@@@@@@@@@@@@@@@@@@@@@
C
C
C          2. CALCULATE THE STRESS INCREMENT,
C             ASSUMING ELASTIC BEHAVIOR
C
30    DELSIG(1) = A1*DELEPS(1) + B1*DELEPS(2)
      DELSIG(2) = B1*DELEPS(1) + A1*DELEPS(2)
      DELSIG(3) = C1*DELEPS(3)
      DELSIG(4) = 0.0D0
      IF (ITYP2D.EQ.2) GO TO 150
      DELSIG(4) = B1 * (DELEPS(1)+DELEPS(2))
      IF (ITYP2D.EQ.1) GO TO 150
      DELSIG(1) = DELSIG(1) + B1*DELEPS(4)
      DELSIG(2) = DELSIG(2) + B1*DELEPS(4)
      DELSIG(4) = DELSIG(4) + A1*DELEPS(4)
C
C
C          3. CALCULATE TOTAL STRESSES,
C             ASSUMING ELASTIC BEHAVIOR
C
150   TAU(4) = 0.0D0
      DO 160 I=1,IST
160   TAU(I) = SIG(I) + DELSIG(I)
C
C          4. CHECK WHETHER *TAU* STATE OF STRESS FALLS
C             OUTSIDE THE LOADING SURFACE
C
      SM = (TAU(1)+TAU(2)+TAU(4))/3.
      SX = TAU(1) - SM
      SY = TAU(2) - SM
      SS = TAU(3)
      SZ = TAU(4) - SM
      IF(JWR.EQ.1)GO TO 170
C
      FT =.5D0*(SX*SX+SY*SY+SZ*SZ) + SS*SS - YLD*YLD/3.D0
C
      IF (FT) 170,170,300
C
C     STATE OF STRESS WITHIN LOADING SURFACE  -  ELASTIC BEHAVIOR
C
170   IPEL=1
      STRESS(4) = 0.0D0
      DO 180 I=1,IST
180   STRESS(I) = TAU(I)
      IF (ITYP2D.EQ.2) STRAIN(4)=EPS(4) + D1*(DELEPS(1) + DELEPS(2))
      IF(JP.GE.2)STRAIN(4)=EPS(4)
      GO TO 400
C
C
```

```
C      STATE OF STRESS OUTSIDE LOADING SURFACE  -  PLASTIC BEHAVIOR
C
C 300 IF (IPEL.EQ.1) GO TO 320
C
C      .......WAS PLASTIC
C
C      IPEL=2
C      RATIO = 0.
C      DO 315 I=1,IST
C 315 TAU(I) = SIG(I)
C      GO TO 370
C
C      .......WAS ELASTIC
C
C      DETERMINE PART OF STRAIN TAKEN ELASTICLY
C
C 320 IPEL=2
300    IPEL=2
C
       SM = (SIG(1)+SIG(2)+SIG(4))/3.0D0
       SX = SIG(1) - SM
       SY = SIG(2) - SM
       SS = SIG(3)
       SZ = SIG(4) - SM
C
       DM = (DELSIG(1)+DELSIG(2)+DELSIG(4))/3.0D0
       DX = DELSIG(1) - DM
       DY = DELSIG(2) - DM
       DS = DELSIG(3)
       DZ = DELSIG(4) - DM
C
       A = DX*DX + DY*DY + 2.0D0*DS*DS + DZ*DZ
       B = SX*DX + SY*DY + 2.0D0*SS*DS + SZ*DZ
       E= SX*SX + SY*SY + 2.0D0*SS*SS + SZ*SZ - 2.0D0*YLD*YLD/3.0D0
C
       RATIO=(-B+SQRT(B*B-A*E))/A
C
       DO 350 I=1,IST
350    TAU(I) = SIG(I) + RATIO*DELSIG(I)
       IF (ITYP2D.EQ.2) STRAIN(4)=EPS(4) + RATIO*D1*(DELEPS(1)
      1+ DELEPS(2))
C
C      *TAU* NOW CONTAINS (PREVIOUS STRESSES +
C      STRESSES DUE TO ELASTIC STRAIN INCREMENTS)
C
C
C         5. CALCULATE PLASTIC STRESSES
C
C      DETERMINE INCREMENT INTERVAL
370    M=20.D0*SQRT(ET)/YLD+1
       IF (M.GT.30) M=30
       XM = (1.D0 - RATIO)/M
C
C
       DO 380 I=1,ISR
380    DEPS(I) = XM*DELEPS(I)
C
C
C      .....  CALCULATION OF ELASTOPLASTIC STRESSES  .....  (START)
C
C***
```

```
C        WRITE(6,2000)
C2000    FORMAT(2X,4HDEPS)
C        WRITE(6,*) (DEPS(I),I=1,4)
C        WRITE(6,*) A,B,E,RATIO
C        WRITE (6,2001)
C2001    FORMAT(2X,3HTAU)
C        WRITE(6,*)(TAU(I),I=1,4)
C***
      DO 600 IM=1,M
C
      CALL MIDEP (TAU,DEPS,C)
C
      DO 560 I=1,IST
      DO 560 J=1,ISR
560   TAU(I) = TAU(I) + C(I,J) * DEPS(J)
C
C
C     CORRECTION
C
      DM = (TAU(1)+TAU(2)+TAU(4))/3.D0
      DX = TAU(1) - DM
      DY = TAU(2) - DM
      DS = TAU(3)
      DZ = TAU(4) - DM
C
      IF (PROP(4).EQ.0.) GO TO 580
C
C     STRAIN-HARDENING MATERIAL -  UPDATE YLD
C
      DP15=1.5D0
      YLD=SQRT  (DP15*(DX*DX+DY*DY+2.*DS*DS+DZ*DZ))
      GO TO 600
C
C     PERFECTLY PLASTIC MATERIAL
C
580   FTA=.5D0*(DX*DX + DY*DY + DZ*DZ) + DS*DS
      FTB=(YLD*YLD)/3.D0
      FT=FTA - FTB
      IF (FT.EQ.0) GO TO 600
      IF (ITYP2D.EQ.2) GO TO 590
C
      COEF=-1.D0 +SQRT(FTB/FTA)
      TAU(1) = TAU(1) + COEF*DX
      TAU(2) = TAU(2) + COEF*DY
      TAU(3) = TAU(3) + COEF*DS
      TAU(4)=TAU(4) + COEF*DZ
      GO TO 600
C
590   COEF=SQRT(FTB/FTA)
      TAU(1)=TAU(1)*COEF
      TAU(2)=TAU(2)*COEF
      TAU(3)=TAU(3)*COEF
      STRAIN(4)=STRAIN(4) + (COEF - 1.D0)*DM/BM
C
600   CONTINUE
C
C     ..... CALCULATION OF ELASTOPLASTIC STRESSES ..... ( END )
C
      STRESS(4) = 0.D0
      DO 390 I=1,IST
390   STRESS(I) = TAU(I)
```

```
C
C
C        6. UPDATING STRESSES, STRAINS, YIELD, NS
C
400     DO 410 I=1,IST
410     SIG(I) = STRESS(I)
        DO 420 I=1,ISR
420     EPS(I) = STRAIN(I)
        YIELD = YLD
        IF (ITYP2D.EQ.2) EPS(4)=STRAIN(4)
        IF (KPRI.EQ.0) GO TO 700
C
C
        IF (ICOUNT.EQ.3) RETURN
C
C          7. FORM THE MATERIAL LAW
C
        IF (IPEL.EQ.1) GO TO 450
C
C       ELASTO-PLASTIC
        CALL MIDEP (TAU,DEPS,C)
C****
C         WRITE(6,3002)
C3002       FORMAT(5X,15HTAU,DEPS,C(I,J))
C         WRITE(6,*) (TAU(I),I=1,4)
C         WRITE(6,*) (DEPS(I),I=1,4)
C         WRITE(6,*) ((C(I,J),J=1,4),I=1,4)
C***
        RETURN
C
C       ELASTIC
450     DO 460 I=1,ISR
        DO 460 J=1,ISR
460     C(I,J)=0.D0
C
C
C       MODIFICATION OF STRESS-STRAIN MATRIX
C       FOR WRINKLED BEHAVIOR
C
C @@@@@@@@@@@@@@@@@@@@@@@@@@@@@@@@@@@@@@@@@@@@@
        IF(JP.NE.2) GO TO 36
          DO 40 I=1,3
          DO 40 J=1,3
40        C(I,J)=0.000100
          RETURN
36      IF(JP.NE.3)GO TO 35
        C(1,1)=P1
        C(1,2)=0.0D0
        C(2,1)=0.0D0
        C(1,3)=Q1
        C(3,1)=Q1
        C(2,2)=P2
        C(2,3)=Q1
        C(3,2)=Q1
        C(3,3)=Q2
        RETURN
C @@@@@@@@@@@@@@@@@@@@@@@@@@@@@@@@@@@@@@
35      C(1,1)=A1
        C(2,1)=B1
        C(1,2)=B1
        C(2,2)=A1
```

```
      C(3,3)=C1
C     IF (ITYP2D.NE.0) RETURN
      IF (ITYP2D.EQ.1) RETURN
      IF (ITYP2D.EQ.2)GO TO 470
      C(1,4)=B1
      C(2,4)=B1
      C(4,1)=B1
      C(4,2)=B1
      C(4,4)=A1
C
      RETURN
C
470   C(4,1)=B2
      C(4,2)=B2
      C(4,3)=0.D0
      C(4,4)=A2
C
      RETURN
C
C
C     P R I N T I N G   O F   S T R E S S E S
C
700   IF (IPEL.EQ.1) GO TO 705
C
      DM=(STRESS(1) + STRESS(2) + STRESS(4))/3.0D0
      DX=STRESS(1) - DM
      DY=STRESS(2) - DM
      DS=STRESS(3)
      DZ=STRESS(4) - DM
      FT=.5D0*(DX*DX + DY*DY + DZ*DZ) + DS*DS - YLD*YLD/3.0D0
C
705   IF (INDNL.NE.2) GO TO 800
C
C     IN TOTAL LAGRANGIAN FORMULATION,
C     CAUCHY STRESSES ARE CALCULATED AND PRINTED
C
      CALL CAUCHY
C
800   IF (NG.NE.NGLAST) GO TO 802
      IF (NEL.GT.NELAST) GO TO 806
      IF (IPT-1) 810,808,810
C
802   NGLAST = NG
808   IF (ITYP2D) 803,805,803
803   IF (IPS.NE.2)
     *WRITE (6,2002)
      GO TO 806
805   IF(IPS.NE.0)
     *WRITE (6,2003)
C
806   NELAST=NEL
      IF(IPS.NE.0)
     *WRITE (6,2004) NEL
810   CALL MAXMIN (STRESS,SX,SY,SM)
      IF (ITYP2D) 813,815,813
C
813   IF (JWR.EQ.1) GO TO 817
      IF (IPS.NE.0)
     *WRITE (6,2005) IPT,STATE(IPEL),
     1(STRESS(I),I=1,3),SX,SY,SM,FT
      GO TO 818
```

```
      IF(JP.EQ.1.AND.IPS.NE.0)
817  *WRITE (6,2013) IPT,STATE(IPEL),(STRESS(I),I=1,3),SX,SY,SM
      IF (IPS.NE.)).AND.JP.EQ.2)
820  *WRITE(6,2005) IPT,(STRESS(I),I=1,3),SX,SY,SM
      IF (IPS.NE.).AND.JP.EQ.3)
     *WRITE(6,2009) IPT,(STRESS(I),I=1,3),SX,SY,SM
      FT=0.000
818   IF (IPES.NE.0)
     *WRITE(18,2010) TIME,NG,NEL,IPT,(STRESS(I),I=1,3),SX,SY,
     1SM,FT,JP
      RETURN
C
815   IF(IPS.NE.0)
     *WRITE (6,2007) IPT,STATE(IPEL),STRESS(4),
     1(STRESS(I),I=1,3),SX,SY,SM,FT
      IF (IPES.NE.0)
     *WRITE(18,2010) TIME,NG,NEL,IPT,STRESS(4),(STRESS(I),I=1,3),
     2SX,SY,SM,FT,JP
8151  CONTINUE
      RETURN
C
C
2002  FORMAT(50H ELEMENT  STRESS       STRESS-YY      STRESS-ZZ      ,
     140HSTRESS-YZ        MAX STRESS     MIN STRESS,21X,5HYIELD/
     250H NUM/IPT   STATE                                          ,
     349H                                                ANGLE,9X,
     43HFUNCTION / )
2003  FORMAT(50H ELEMENT  STRESS       STRESS-XX      STRESS-YY      ,
     154HSTRESS-ZX        STRESS-YZ      MAX STRESS     MIN STRESS,
     221X,5HYIELD/33H NUM/IPT   STATE                              ,
     345H                                                          ,
     43HANGLE,9X,8HFUNCTION/)
2004  FORMAT (I4/)
2005  FORMAT (5X,I2,2X,A1,6HLASTIC,1X,3E14.6,3X,2E14.6,3X,F6.2,3X,E14
2013   FORMAT(5X,I2,2X,A1,6HLASTIC,1X,3E14.6,3X,2E14.6,3X,F6.2)
2006  FORMAT (5X,I2,2X,7HSLACK  ,1X,3E14.6,3X,2E14.6,3X,F6.2)
2009  FORMAT (5X,I2,2X,7HWRINKLE,1X,3E14.6,3X,2E14.6,3X,F6.2)
2007  FORMAT (5X,I2,2X,A1,6HLASTIC,1X,4E14.6,3X,2E14.6,3X,F6.2,3X,E14
C
2010  FORMAT(F10.5,3I5,5X,3E14.6/5E14.6,2X,I2)
      END
```

APPENDIX C

SAP 7 INPUT LISTING FOR VERIFICATION EXAMPLE NO. 1

```
***TEST PROBLEM FOR NASA PROJECT
*CONTROL
M1,6D,NL,E
M4,0,0,321
M5,320,0.0625,0.0,4
*LOADS
63,2,3
1,3
0.0,0.0,1.0,0.04,20.0,0.04
2,3
0.0,0.0,1.0,0.0,20.0,0.04
L,192,192,10,2,1,0.003
L,183,191,1,2,1,0.006
L,11,181,170,3,1,0.002
L,17,170,17,3,1,0.008
L,28,164,17,3,1,0.004
L,1,171,170,3,1,-0.002
L,12,165,17,3,1,-0.008
L,18,154,17,3,1,-0.004
L,182,182,1,2,2,-0.014
L,183,183,1,2,2,-0.024
L,184,184,1,2,2,-0.018
L,185,185,1,2,2,-0.012
L,186,186,1,2,2,-0.006
L,188,188,1,2,2,0.006
L,189,189,1,2,2,0.012
L,190,190,1,2,2,0.018
L,191,191,1,2,2,0.024
L,192,192,1,2,2,0.014
*2/D,NL
1,2,3,2,0,9,1
1
7.2E+4,0.333,1.0E+4
*BEAM,L
0,0,1,1,8
1
9.0E+6,0,3.0E+6,0,0
1.0,0.0,0.0,0.0,0.1666667,0.0933333,0.0333333,0.166667,0.166667
*TIE
*MATCH
FINISH
```

```
**TEST PROBLEM FOR NASA PROJECT(MODEL INPUT)
102,71
ECHO
CC START GENERATION OF NODES
NODE,1,0.0,0.0,0.0
TR,10,1,1,1,1,0.0,0.0,0.6
TR,10,1,11,1,17,0.0,1.2,0.0
NODE,12,0.0,0.5,0.0
TR,5,12,12,1,1,0.0,0.0,1.2
TR,9,12,17,1,17,0.0,1.2,0.0
NODE,182,0.0,12.1,0.0
TR,10,182,182,0.1,0.0,0.0,0.6
CC START GENERATION OF BOUNDARY CONDITIONS
FIX,1,1,1,DZ
FIX,1,11,1,DY
FIX,1,181,1,DX,RR
FIX,182,192,1,DX,RY,RZ
CC SAVE NODAL CO-ORDINATES INFORMATIONS
NWRITE
CC START GENERATION OF 2D ELEMENTS
EL,1,2D,1,0.0,0.01,1,8
1,13,20,3,12,19,13,2
REP,9,1,1,1,17
EL,11,2D,1,0.0,0.01,1,8
3,20,22,5,13,21,14,4
REP,9,11,11,1,17
EL,21,2D,1,0.0,0.01,1,8
5,22,24,7,14,23,15,6
REP,9,21,21,1,17
EL,31,2D,1,0.0,0.01,1,8
7,24,26,9,15,25,16,8
REP,9,31,31,1,17
EL,41,2D,1,0.0,0.01,1,8
9,26,23,11,16,27,17,10
REP,9,41,41,1,17
CC SAVE ELEMENT INFORMATIONS
EWRITE
CC START GENERATION OF BEAM ELEMENTS
EL,1,BEAM,182,183,103,1,0,0,0,0.0,1.00
EL,2,B,183,184,104,1,0,0,0,0.0,1.00
EL,3,B,184,185,105,1,0,0,0,0.0,1.00
EL,4,B,185,186,106,1,0,0,0,0.0,1.00
EL,5,B,186,187,107,1,0,0,0,0.0,1.00
EL,6,B,187,188,108,1,0,0,0,0.0,1.00
EL,7,B,188,189,109,1,0,0,0,0.0,1.00
EL,8,B,189,190,110,1,0,0,0,0.0,1.00
EL,9,B,190,191,111,1,0,0,0,0.0,1.00
EL,10,B,191,192,112,1,0,0,0,0.0,1.00
EWRITE
CC START GENERATION OF CONSTRAINTS ELEMENTS
EL,1,CP,1
171,182
REP,4,1,1,1,1
EL,6,CP,1
177,188
REP,4,6,6,1,1
EWRITE
EL,1,CP,1
176,187
EWRITE
END
```

APPENDIX D

SAP 7 INPUT LISTING FOR VERIFICATION EXAMPLE NO. 2

```
**CIRCULAR MEMBRANE(CIRCUMFERANCIAL TP AND SP)FOR NASA PROJECT
*CONTROL
M1,20,NL,F
M4,0,0,241
M5,240,0.0625,0.0,4
*LOADS
0,2,3,0,0,0,48
1,3
0.0,0.0,1.0,0.02,15.0,0.02
2,3
0.0,0.0,1.0,0.0,15.0,0.02
P2D,7,18,11,0,2,1,2,0.0,0.5,0.01
P2D,18,29,22,0,2,1,2,0.5,0.866025,0.01
P2D,29,40,33,0,2,1,2,0.866025,1.0,0.01
P2D,40,51,44,0,2,1,2,1.0,0.866025,0.01
P2D,51,62,55,0,2,1,2,0.866025,0.5,0.01
P2D,62,73,66,0,2,1,2,0.5,0.0,0.01
P2D,73,84,77,0,2,1,2,0.0,-0.5,0.01
P2D,84,95,88,0,2,1,2,-0.5,-0.866025,0.01
P2D,95,106,99,0,2,1,2,-0.866025,-1.0,0.01
P2D,106,117,110,0,2,1,2,-1.0,-0.866025,0.01
P2D,117,128,121,0,2,1,2,-0.866025,-0.5,0.01
P2D,128,7,132,0,2,1,2,-0.5,0.0,0.01
P2D,7,18,11,0,1,1,2,1.0,0.866025,0.01
P2D,18,29,22,0,1,1,2,0.866025,0.5,0.01
P2D,29,40,33,0,1,1,2,0.5,0.0,0.01
P2D,40,51,44,0,1,1,2,0.0,-0.5,0.01
P2D,51,62,55,0,1,1,2,-0.5,-0.866025,0.01
P2D,62,73,66,0,1,1,2,-0.866025,-1.0,0.01
P2D,73,84,77,0,1,1,2,-1.0,-0.866025,0.01
P2D,84,95,88,0,1,1,2,-0.866025,-0.5,0.01
P2D,95,106,99,0,1,1,2,-0.5,0.0,0.01
P2D,106,117,110,0,1,1,2,0.0,0.5,0.01
P2D,117,128,121,0,1,1,2,0.5,0.866025,0.01
P2D,128,7,132,0,1,1,2,0.866025,1.0,0.01
P2D,7,18,11,0,2,2,2,1.0,0.866025,0.01
P2D,18,29,22,0,2,2,2,0.866025,0.5,0.01
P2D,29,40,33,0,2,2,2,0.5,0.0,0.01
P2D,40,51,44,0,2,2,2,0.0,0.5,0.01
P2D,51,62,55,0,2,2,2,0.5,0.866025,0.01
P2D,62,73,66,0,2,2,2,0.866025,1.0,0.01
P2D,73,84,77,0,2,2,2,1.0,0.866025,0.01
P2D,84,95,88,0,2,2,2,0.866025,0.5,0.01
P2D,95,106,99,0,2,2,2,0.5,0.0,0.01
P2D,106,117,110,0,2,2,2,0.0,-0.5,0.01
P2D,117,128,121,0,2,2,2,-0.5,-0.866025,0.01
P2D,128,7,132,0,2,2,2,-0.866025,-1.0,0.01
P2D,7,18,11,0,1,2,2,0.0,0.5,0.01
P2D,18,29,22,0,1,2,2,0.5,0.866025,0.01
P2D,29,40,33,0,1,2,2,0.866025,1.0,0.01
P2D,40,51,44,0,1,2,2,1.0,0.866025,0.01
P2D,51,62,55,0,1,2,2,0.866025,0.5,0.01
P2D,62,73,66,0,1,2,2,0.5,0.0,0.01
P2D,73,84,77,0,1,2,2,0.0,-0.5,0.01
P2D,84,95,88,0,1,2,2,-0.5,-0.866025,0.01
P2D,95,106,99,0,1,2,2,-0.866025,-1.0,0.01
P2D,106,117,110,0,1,2,2,-1.0,-0.866025,0.01
P2D,117,128,121,0,1,2,2,-0.866025,-0.5,0.01
P2D,128,7,132,0,1,2,2,-0.5,0.0,0.01
*P2D,NL
1,2,8,2,0,9,1


1
7.2E+4,0.333,1.0E+4
FINISH
```

```
##CIRCULAR MEMBRANE(CIRCUMFERANCIAL T AND S)FOR NASA
1,2,36
ECHO
CC GENERATE NODES
NODE,1,0.0,20.0,0.00
TR,5,1,1,1,1,0.0,10.0,0.0
ROT,1,1,1,1,7,-15.0,X
ROT,1,3,3,1,6,-15.0,X
ROT,1,5,5,1,5,-15.0,X
ROT,1,7,7,1,4,-15.0,X
ROT,11,1,7,1,11,-30.0,X
ROT,11,8,11,1,11,-30.0,X
CC GENERATE B.CONDITIONS
FIX,1,122,11,DY,DZ
FIX,8,129,11,DY,DZ
NWRITE
CC GENERATE ELEMENTS
ELE,1,20,1,0,1.0E-2,1,8
14,12,1,3,13,8,2,9
ELE,2,20,1,0,1.0E-2,1,8
16,14,3,5,15,9,4,10
ELE,3,20,1,0,1.0E-2,1,8
18,16,5,7,17,10,6,11
RE,10,1,3,1,11
EL,34,20,1,0,1.0E-2,1,8
3,1,122,124,2,129,123,130
EL,35,20,1,0,1.0E-2,1,8
5,3,124,126,4,130,125,131
EL,36,20,1,0,1.0E-2,1,8
7,5,126,128,6,131,127,132
EWRITE
END
```

1. Report No.	2. Government Accession No.	3. Recipient's Catalog No.
NASA CR-172325		

4. Title and Subtitle	5. Report Date
Finite Element Analysis of Wrinkling Membranes	April 1984
	6. Performing Organization Code

7. Author(s)	8. Performing Organization Report No.
Richard K. Miller, John M. Hedgepeth*, Victor I. Weingarten, Prasanta Das, and Shahrzad Kahyai	USC-CE-83-05
	10. Work Unit No.

9. Performing Organization Name and Address	11. Contract or Grant No.
Dept. of Civil Engineering U. of Southern California Los Angeles, CA 90089	NAG1-235
	13. Type of Report and Period Covered
12. Sponsoring Agency Name and Address	Contractor Report
National Aeronautics and Space Administration Washington, DC 20546	14. Sponsoring Agency Code

15. Supplementary Notes

Langley Technical Monitor: Dr. Wilbur B. Fichter
*Consultant, Astro Research Corporation, Carpinteria, California

16. Abstract

The development of a nonlinear numerical algorithm for the analysis of stresses and displacements in partly wrinkled flat membranes, and its implementation on the SAP VII finite-element code are described. A comparison of numerical results with exact solutions of two benchmark problems reveals excellent agreement, with good convergence of the required iterative procedure. Also reported is an exact solution of a problem involving axisymmetric deformations of a partly wrinkled shallow curved membrane.

17. Key Words (Suggested by Author(s))	18. Distribution Statement
Membranes Wrinkling Finite element	Unclassified - Unlimited Subject Category 39

19. Security Classif. (of this report)	20. Security Classif. (of this page)	21. No. of Pages	22. Price
Unclassified	Unclassified	85	A05

For sale by the National Technical Information Service, Springfield, Virginia 22161